

THE
IIOAB
JOURNAL

VOLUME 7 : NO 1 : APRIL 2016 : ISSN 0976-3104



Institute of Integrative Omics and
Applied Biotechnology Journal

Dear Esteemed Readers, Authors, and Colleagues,

I hope this letter finds you in good health and high spirits. It is my distinct pleasure to address you as the Editor-in-Chief of Integrative Omics and Applied Biotechnology (IIOAB) Journal, a multidisciplinary scientific journal that has always placed a profound emphasis on nurturing the involvement of young scientists and championing the significance of an interdisciplinary approach.

At Integrative Omics and Applied Biotechnology (IIOAB) Journal, we firmly believe in the transformative power of science and innovation, and we recognize that it is the vigor and enthusiasm of young minds that often drive the most groundbreaking discoveries. We actively encourage students, early-career researchers, and scientists to submit their work and engage in meaningful discourse within the pages of our journal. We take pride in providing a platform for these emerging researchers to share their novel ideas and findings with the broader scientific community.

In today's rapidly evolving scientific landscape, it is increasingly evident that the challenges we face require a collaborative and interdisciplinary approach. The most complex problems demand a diverse set of perspectives and expertise. Integrative Omics and Applied Biotechnology (IIOAB) Journal has consistently promoted and celebrated this multidisciplinary ethos. We believe that by crossing traditional disciplinary boundaries, we can unlock new avenues for discovery, innovation, and progress. This philosophy has been at the heart of our journal's mission, and we remain dedicated to publishing research that exemplifies the power of interdisciplinary collaboration.

Our journal continues to serve as a hub for knowledge exchange, providing a platform for researchers from various fields to come together and share their insights, experiences, and research outcomes. The collaborative spirit within our community is truly inspiring, and I am immensely proud of the role that IIOAB journal plays in fostering such partnerships.

As we move forward, I encourage each and every one of you to continue supporting our mission. Whether you are a seasoned researcher, a young scientist embarking on your career, or a reader with a thirst for knowledge, your involvement in our journal is invaluable. By working together and embracing interdisciplinary perspectives, we can address the most pressing challenges facing humanity, from climate change and public health to technological advancements and social issues.

I would like to extend my gratitude to our authors, reviewers, editorial board members, and readers for their unwavering support. Your dedication is what makes IIOAB Journal the thriving scientific community it is today. Together, we will continue to explore the frontiers of knowledge and pioneer new approaches to solving the world's most complex problems.

Thank you for being a part of our journey, and for your commitment to advancing science through the pages of IIOAB Journal.



Yours sincerely,

Vasco Azevedo

Vasco Azevedo, Editor-in-Chief
Integrative Omics and Applied Biotechnology
(IIOAB) Journal



Prof. Vasco Azevedo
Federal University of Minas Gerais
Brazil

Editor-in-Chief

Integrative Omics and Applied Biotechnology (IIOAB) Journal Editorial Board:



Nina Yiannakopoulou
Technological Educational Institute of Athens
Greece



Jyoti Mandlik
Bharati Vidyapeeth University
India



Rajneesh K. Gaur
Department of Biotechnology, Ministry of Science and Technology
India



Swarnalatha P
VIT University
India



Vinay Aroskar
Sterling Biotech Limited
Mumbai, India



Sanjay Kumar Gupta
Indian Institute of Technology
New Delhi, India



Arun Kumar Sangaiah
VIT University
Vellore, India



Sumathi Suresh
Indian Institute of Technology
Bombay, India



Bui Huy Khoi
Industrial University of Ho Chi Minh City
Vietnam



Tetsuji Yamada
Rutgers University
New Jersey, USA



Moustafa Mohamed Sabry Bakry
Plant Protection Research Institute
Giza, Egypt



Rohan Rajapakse
University of Ruhuna
Sri Lanka



Atun RoyChoudhury
Ramky Advanced Centre for Environmental Research
India



N. Arun Kumar
SASTRA University
Thanjavur, India



Bui Phu Nam Anh
Ho Chi Minh Open University
Vietnam



Steven Fernandes
Sahyadri College of Engineering & Management
India

MULTI - KEYWORD RANKED SEARCH OVER ENCRYPTED DATA SUPPORTING SYNONYM QUERY

Jayanthi M.* and Prabadevi

School of Information Technology and Engineering, VIT University, Vellore, TN, INDIA

ABSTRACT

With the advantage of storage as a service many enterprises are moving their valuable data to the cloud, since it costs less, easily scalable and can be accessed from anywhere any time. The trust between cloud user and provider is paramount. We use security as a parameter to establish trust. Cryptography is one way of establishing trust. Searchable encryption is a cryptographic method to provide security. In literature many researchers have been working on developing efficient searchable encryption schemes. In this paper we explore some of the effective cryptographic techniques based on vector space model (VSM), which manages increased control complexity of the data centre, and a less efficient cloud storage system.

Received on: 6th-May-2015

Revised on: 2nd-Sept-2015

Accepted on: 17th-Sept-2015

Published on: 5th-Jan-2016

KEY WORDS

Vector space model, cloud service provider, term frequency, inverse document frequency

*Corresponding author: Email: jayanthimurali93@gmail.com Tel: +91-9894716850

INTRODUCTION

Cloud Computing paradigm provides a variety of service to the consumers. Many consumer electronic devices (e.g. Smartphone) with support of high speed computing combined with the emerging cloud. A cloud computing middleware Media Cloud for set top boxes for classifying, searching, and delivering media inside home network and across the cloud [1].

One hand, consumer-centric cloud computing a new model of enterprise-level IT infrastructure that provides on demand high quality applications and services from a shared pool of configuration computing resources for consumers. On the other hand, some problems may be caused in this circumstance since the Cloud Service Provider (CSP) possesses full control of the outsourced data. Sensitive data are encrypted before outsourcing to the cloud.

However, encrypted data make the traditional data utilization services based on plaintext keyword search useless [2]. The simple and embarrassed method of downloading all the data and decrypting locally is obviously impractical, because the authorized cloud consumers must hope to search their interested data rather than all the data

MATERIALS AND METHODS

Multi keyword ranked search

The existing systems like exact or fuzzy keyword search, supports only single keyword search. These schemes doesn't retrieve the relevant data to users query therefore multi-keyword ranked search over encrypted cloud data remains a very challenging problem. To meet this challenge of effective search system, an effective and flexible searchable scheme is proposed that supports multi-keyword ranked search [3]. To address multi-keyword search and result ranking, Vector Space Model (VSM) is used to build document index, each document is expressed as a vector where each dimension value is the Term Frequency (TF) weight of its corresponding keyword. A new vector is also generated in the query phase. The vector has the same dimension with document index and its each dimension value is the Inverse Document Frequency (IDF) weight. Then cosine measure can be used to compute similarity of one document to the search query. To improve search efficiency, a tree-based index structure used which is a balance binary tree is. The searchable index tree is constructed with the document index vectors. So the related documents can be found by traversing the tree.

Synonym search

While user searching the data on cloud server it might be possible that the user is unaware of the exact words to search, i.e. there is no tolerance of synonym substitution or syntactic variation which are the typical user searching behaviors and happen very frequently [4]. To solve this problem semantic based search method is used. To improve the search for information it is necessary that search engines can understand what the user wants so they are able to answer objectively. To achieve that, one of the necessary things is that the resources have information that can be helpful to searches.

The Semantic Web proposed to clarify the meaning of resources by annotating them with metadata data over data [5]. By associating metadata to resources, semantic searches can be significantly improved when compared to traditional searches. It allows users the use of natural language to express what he wants to find [6]. Here the enhanced VSM algorithm is proposed for improving documental searches optimized for specific scenarios where user want to find a document but don't remember the exact words used, if plural or singular words were used or if a synonym was used.

The defined algorithm takes into consideration:

- 1) The number of direct words of the search expression that are in the document;
- 2) The number of word variation of the search expression that are in the document;
- 3) The number of synonyms of the words in the search expression that are in the document.

Vector space model algorithm

Vector space model is an algebraic model for representing text documents (and any objects, in general) as vectors of identifiers, for example, index terms. It is used in information filtering, information retrieval, indexing and relevancy rankings. To address multi-keyword search and result ranking, Vector Space Model (VSM) is used to build document index, each document is expressed as a vector where each dimension value is the Term Frequency (TF) weight of its corresponding keyword. A new vector is also generated in the query phase [7].

RESULTS

Our system consists of 3 entities viz., data owner, data user and the cloud server as shown in **Figure- 1**.

Data owner

1. Encrypts the data files for securing the data in cloud before uploading into the cloud.
2. They define the access rights for the user who want to access those documents.
3. The access right is a 2-state variable: permission granted or permission denied.

Cloud server

1. Stores the encrypted data files and encrypted index tree.
2. It accepts the encrypted keywords and returns the matching data file based on their relevance.

Data user

1. User can search for encrypted data files in cloud with encrypted keywords.
2. The purpose of using encrypted keywords is that even the cloud server must not be able to infer the contents of data files.

This system is implemented in **ASP. NET** framework using **C#** and the process includes the following:

1. The data owner uploads the text files (documents) in cloud storage. Once the files get uploaded the owner is generating the encryption key through which the uploaded files are encrypted and are available only for the authorized users.
2. The registered data users can search the interesting data and can request the key from the data owner to download the document. The system matches the partial substring or various synonyms of the actual document name in the storage. For example, consider a document named Model.doc is uploaded in the cloud storage. The user query strings such as form, plan, and mod will be matched for the string "Model" and the document Model.doc will be retrieved. Through which Multi-Keyword searching is achieved.
3. Data owner forwards the decryption key to the secured user to access the documents; else the pop up error message will arise when the document is accessed without decryption key request made by the respective user.

File uploading

In the new system we build a secure index and outsource it along with the encrypted data items. Each index is mapped to a data bucket. Data bucket contain id of all the documents which have the bucket index as one of its index. At time of document upload the client send a request to the server for a unique password. Then the server generate the password form the features of document and how uploading the document and send to the client/data owner. Then using that password the data owner encrypt the document and uploaded the document along with the secure indexes [8].

At the time of file upload the server check for corresponding bucket in the data base based on the index word given by the user and selects the corresponding bucket to a data item. If there is no such a bucket then the server creates a new bucket for the documents index and adds the document to the newly created bucket. The password generation module which generates the unique password for the document provides extra security. The password generation consists of message digest creation using SHA-1 and converts the 160 bit message digest to 128 bit key for encryption [9].

The data owner’s unique identifier, the file’s unique identifier and the file name are used to generate the message digest. The AES is the encryption scheme used to encrypt the files. Based on the words inside the document the system itself able to predict the index words, but the final submission is by the data owner. He can select from the predicted words by the system or can add manually and the figure for this is shown in **figure-2** File uploading.

Files searching

Search is performed based on the all the synonyms and search words across bucket indexes and return all the authorized documents corresponding to from the selected buckets. The results are ranked based on the history and the number of times the document id is present in the buckets. That is it support for multi-key word search and then returns the best result as the first document and the figure for this is shown in **figure-2** File searching

Files downloading

The input to the SHA-1 is the data owner’s unique identifier, the file’s unique identifier and the file name. Then the 160 bit is converted to 128 bit and the 128 bit key is used for the AES decryption. The file and the key are given to the client and the decryption is performed in the client side and the figure for this is shown in **figure-2** File Downloading.

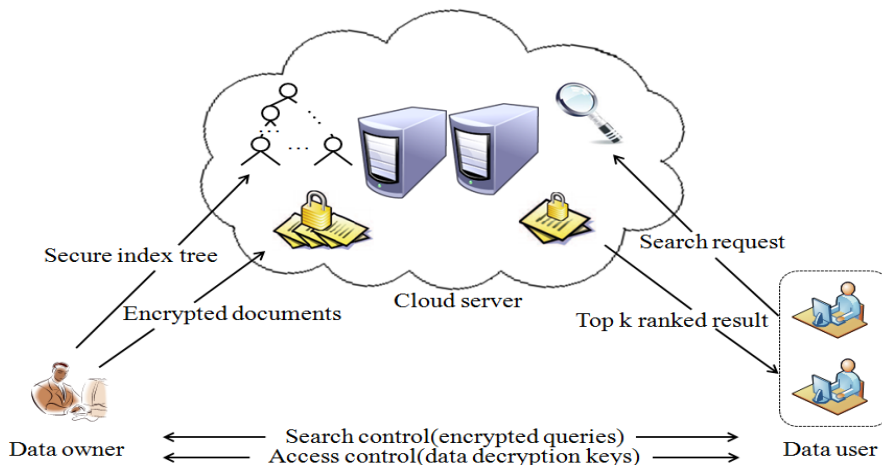


Fig: 1. Searchable encryption architecture using vsm

A

B

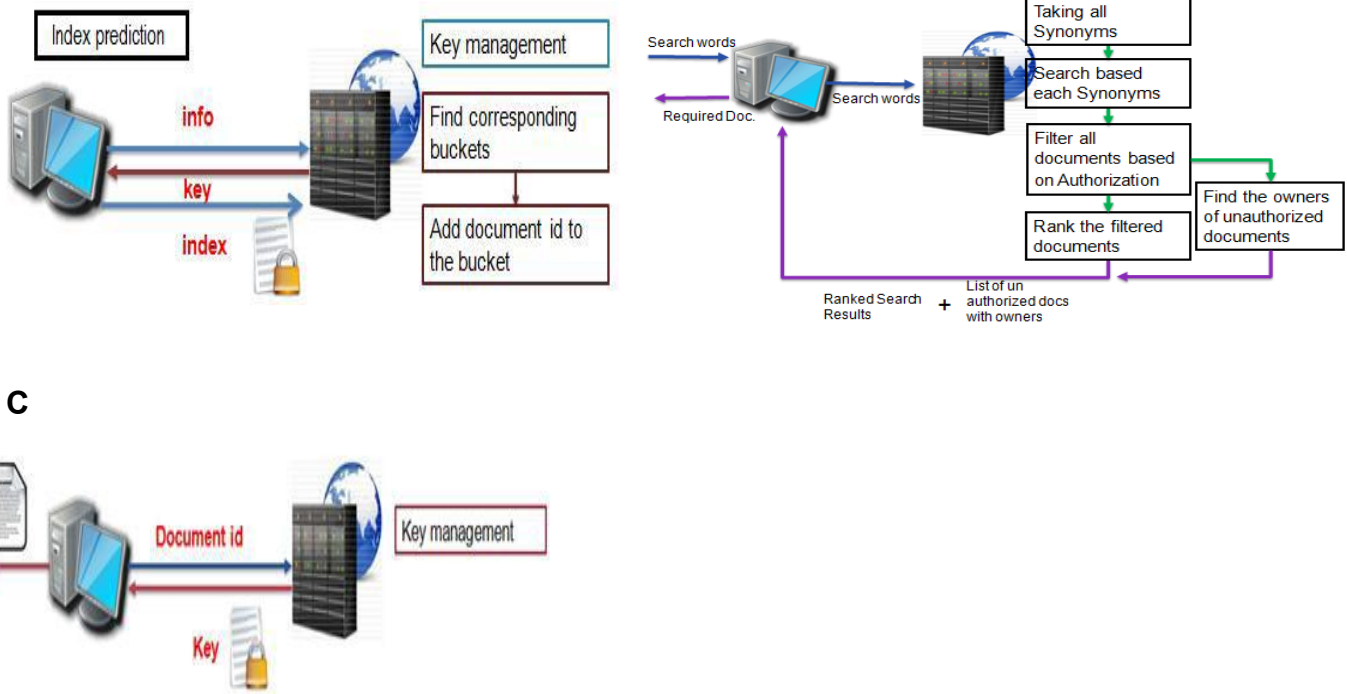


Fig: 2. File uploading, searching, downloading

DISCUSSION

Here we present the experimental evaluation of the Synonym based Ranked Secure Search over Encrypted Data. We investigated the success of our proposed scheme in the context of user unaware key management, automatic index prediction; synonym based searching, multi-key word search, user authentication and document ranking. For the purpose of testing we constructed a database of 200 documents entries.

User unaware key management

To verify the user unaware key management we want to evaluate mainly 2 things. First one is the uniqueness of the key. The second is the same key generation at the time of encryption and decryption. First one is evaluated using uploading same document with same indexes by same and different data owners [10]. And the result is checked by performing search on the data base for any two similar encrypted documents. 10 data owners are uploaded the same document 5 times but cannot find the similar encrypted files in the data base. The rest is evaluated by downloading random 100 documents and check they are perfectly decrypted or not. We observed that all are decrypted correctly.

Automatic index prediction

The automatic index prediction is evaluated by checking the predicted indexes and keywords of the documents. Testing is done with 20 document files, 20 text files, 20 PDF file. The most frequent words, which may consider as the candidate for the index, are successfully predicted by the system [11].

Search Performance based on number of documents in each bucket

The performance of the system is checked by testing the execution time of the search with different indexes which have various numbers of documents inside each index bucket [11]. The number of documents in each bucket is denoted. At the starting the search time is increased with increasing number of documents inside the bucket. But later it become almost constant.

CONCLUSION

The energy efficiency is the important key Wireless sensor networks. With data transmission is the major part of energy consumption, chaos theory based time series prediction method to enhance energy efficiency. The proposed Chaos Theory based Data Aggregation (CTAg) based approach reduces redundant data, communication overhead and number of packet transmission between aggregator and sink node by using adaptive thresholds. The time series prediction using CTAg method was energy efficient and performed less computation to obtain the forecasted data. The experiments also show CTAg achieves better performance compared to other prediction approaches like Kalman Filter [KF] based prediction.

CONFLICT OF INTEREST

The author declares having no competing interests.

ACKNOWLEDGEMENT

We are thankful to VIT University for providing necessary resources for successfully implementation of this system

FINANCIAL DISCLOSURE

No financial support was received for this implementation.

REFERENCES

- [1] Almeearas. [2014] Achieving Effective Cloud Search Services Multi-keyword Ranked Search over Encrypted Cloud Data Supporting Synonym Query- *IEEE Transactions on Consumer Electronics- 2014*
- [2] R Sanchez, P Arias, D Diaz-Sanchez, and A Marin. [2012] Enhancing privacy and dynamic federation in IdM for consumer cloud computing, *IEEE Trans. Consumer Electron* 58(1): 95–103.
- [3] Chai and G Gong. [2012] Verifiable symmetric searchable encryption for semi-honest-but-curious cloud servers, Proceedings of (ICC'12), *IEEE International Conference on Communications* pp. 917–922.
- [4] PA Cabarcos, FA Mendoza, RS Guerrero, AM Lopez, D Diaz-Sanchez. [2012] SuSSo: seamless and ubiquitous single sign-on for cloud service continuity across devices, *IEEE Trans. Consumer Electron* 58(4): 1425–1433.
- [5] D Diaz-Sanchez, F Almenarez, A Marin, D Presario, PA Cabarcos. [2011] Media cloud: an open cloud computing middleware for content management, *IEEE Trans. Consumer Electron*, 57(2): 970–978.
- [6] S Grzonkowski, PM Corcoran. [2011] Sharing cloud services: user authentication for social enhancement of home networking, *IEEE Trans. Consumer Electron*, 57(3): 1424–1432.
- [7] J Li, Q Wang, C Wang, N Cao, K Ren, W Lou. [2010] Fuzzy keyword search over encrypted data in cloud computing, *Proceedings of IEEE INFOCOM'10 Mini-Conference, San Diego, CA, USA*, pp. 1–5, Mar.
- [8] C Wang, N Cao, J Li, K Ren, and W Lou. [2010] Secure ranked keyword search over encrypted cloud data, Proceedings of *IEEE 30th International Conference on Distributed Computing Systems (ICDCS)*, 253–262.
- [9] SG Lee, D Lee, and S Lee. [2010] Personalized DTV program recommendation system under a cloud computing environment," *IEEE Trans. Consumer Electron.*, 56(2):1034–1042.
- [10] N Cao, C Wang, M Li, K Ren, and W Lou. [2011] Privacy-preserving multi keyword ranked search over encrypted cloud data," Proceedings of *IEEE INFOCOM 2011*, 829–837.
- [11] Chai, G Gong. [2012] Verifiable symmetric searchable encryption for semi-honest-but-curious cloud servers, Proceedings of *IEEE International Conference on Communications (ICC'12)*, 917–922.
- [12] R Sanchez, P Arias, D Diaz-Sanchez, A Marin. [2012] Enhancing privacy and dynamic federation in IdM for consumer cloud computing," *IEEE Trans. Consumer Electron.*, 58(1): 95–103.



Jayanthi M. is currently associated with School of Information and Technology, VIT, Vellore, India. She is now pursuing M.S. in Software Engineering. Her area of interest is Cloud Computing, Data Mining.



Prof. Prabadevi is working as an Assistant Professor in the School of Information and Technology, VIT University, Vellore. She has completed her Undergraduate and post graduation under Anna University, Chennai and currently pursuing her Ph.D at VIT University, in the area of Security in Cloud Computing.

A MULTI-STAGE HYBRID CAD APPROACH FOR MRI BRAIN TUMOR RECOGNITION AND CLASSIFICATION

Aju*and Rajkumar

School of Computing Science and Engineering, VIT University, Vellore, TN, INDIA

ABSTRACT

Brain tumor is one of the acute diseases that happen to humans and it is the major reasons of death amid all other types of the cancers. Appropriate and timely diagnosis can prolong the death of a person to some extent. Therefore, an automated and reliable computer-aided diagnostic system for diagnosing and classifying the brain tumor has been proposed. The proposed method is a multi-stage diagnostic system that recognizes and classifies the brain tumor effectively. First, a pre-processing step is performed for both T1-weighted and T2-weighted MR images. The T1-weighted image is sharpened for improving the brightness of its edges. Subsequently, the T2-weighted image is filtered for noise removal and edge retention using trilateral filtering. The sharpened T1-weighted image and the filtered T2-weighted image are blended together to obtain a single improved MR image. Secondly, the improved MR image is segmented using a hybrid segmentation process of skull stripping and enhanced watershed segmentation for extracting the tumor regions. Finally, the extracted tumor is classified using support vector machine to determine whether the tumor is benign or malignant. The results of the proposed system is promising and shows that the extracted brain tumor is better than the ground truth images in most of the cases. Also, the proposed system was able to achieve an accuracy of 94% in classifying the extracted tumor. Hence, the proposed computer-aided diagnostic system can effectively enhance the diagnostic capabilities of physicians with reduced time.

Received on: 2nd-Oct-2015

Revised on: 13th-Nov-2015

Accepted on: 18th-Nov-2015

Published on: 10th-Jan-2016

KEY WORDS

CAD, Enhanced Watershed Segmentation, Support Vector Machine, Skull-Stripping.

*Corresponding author: Email: daju@vit.ac.in Tel: +91-9042250288

INTRODUCTION

Brain tumor is one of the most common and major source of death around the world. Always, early detection of brain tumor is a very hectic and challenging task. Brain tumor may appear clear in Magnetic Resonance Imaging than the other types of imaging. The MRI provides better information on soft tissues and significantly improves the understanding of the normal and the diseased anatomy of the brain. Image contrast is the main purpose of all imaging methods and it allows us to differentiate the brain structures. It also determines which brain structures are normal and which structures are abnormal.

MRI structural contrast is superior to the structural contrast present in other imaging modalities. In MRI, tissue relaxation properties greatly influence image contrast. The two relaxation properties in MR imaging is T1 relaxation and T2 relaxation. The T1-weighted imaging is used to discern the structures based on the T1 values and the T2-weighted imaging discerns the structures based on the T2 values. Tissues with high fat content appear bright and the partitions filled with water appears dark in T1-weighted image. And in T2-weighted images, the partitions filled with water will appear bright and the tissues with high fat content will appear dark. The developed CAD system exploits both these weighted images to segment the tumor and classify whether it is benign or malignant. Further, image processing techniques applied to MRI can cater greater help in probing and diagnosing the brain tumor.

RELATED WORKS

A comprehensive overview and comparison of brain tumors in MR imaging [1], [2] is provided and the pre-processing operations and a futuristic method for brain tumor segmentation is introduced. Also, the evaluation and the validation of the obtained segmented results are presented based upon its efficiency. Various clustering techniques [3] were utilized and implemented to extract and specify the tumor area in a MR image. The classification in the executed methodology confirms whether the tumor is benign or malignant. A three stage approach [4] for diagnosing the brain tumor identifies and segregates the tumor and is invariant in terms of size,

shape and intensity of the tumor. The histogram equalization and morphological processing based CAD system [5] is described. Experimentation is carried out with the help of 125 MR images from 8 persons having tumor and 3 persons without tumors. Six classification algorithms are compared to each other for its efficiency and the authors claim that particle swarm optimization SVM with KNN delivers 100% attainment with their developed system.

Detection and analysis of brain tumor [6] by a novel multi-stage method deals with three brain tumor types such as HG gliomas, metastases and meningioma's. The developed method is experimented for segmenting and accessing the brain tumor with FLAIR, T1-Weighted, Contrast Enhanced T1-Weighted and Perfusion Weighted Image modalities. A brain tumor extraction method [7] reduces the noise and retains the edges in the MRI T2-weighted images. Morphological operations are utilized and manipulated with four different methodologies for extracting and calculating the area of the mass of tissue region.

A fully automated brain tumor detection system [8] aims to determine whether the given T2-weighted MR image has tumor or not and localize it. The developed system was experimented with 131 healthy and 72 tumor affected brain images of T2-weighted MRI modality. The system was able to register an efficiency rate of 95.83 % of correct anomaly detection and 87 % of correct tumor location. A segmentation and automatic tumor class identification methodology [9] is proposed based on a statistical approach assisted by probability maps. The developed system is compared and evaluated with the BRATS (BRAIn Tumor Segmentation) and Leaderboard dataset which encouragingly gave improved results. It is interestingly found that the (GHMRF) Gaussian Hidden Markov Random Field approach attained first in the overall test ranking.

A statistical approach algorithm [10-12] is designed for analyzing the MRI brain images that extracts the data related to brain tumor and locates the tumor. The segmented images are made use of for constructing a 3D model of the tumor region. Various texture features are extracted from the T1-weighted and T2-weighted MR image and classified to find the pathological deficiency in the image. A novel technique for Glioblastoma feature extraction [13] extracts the Gaussian mixture model (GMM) features utilizing the T1-weighted, T2-weighted and Fluid-Attenuated Inversion Recovery (FLAIR) MR images and yields 97.05 % of high accuracy with the classification. A classification system [14] classifies the brain cancer using Principal Component Analysis (PCA) and Back Propagation Neural Network (BPNN) influencing the Gray Level Co-occurrence matrix features. A spatial fuzzy clustering method segments and analyses [15] the structure of MRI brain for segregating the normal tissues and the abnormal tissues of the brain by the enhanced image fusion technique through fuzzy c-means algorithm.

The work carried out by all the aforementioned authors were unique in their own way and they were able to achieve better results. Even though few authors were able to work with different modalities of imaging, none of them were able to capitalize by manipulating the T1-weighted and T2-weighted MR images. Evidently, the proposed system uses and manipulates both the T1-weighted and T2-weighted MR images which helps in segmenting and diagnosing the tumor in an efficient manner. Moreover, an enhanced watershed segmentation algorithm is utilized in the proposed system to extract the brain tumor in an effective way.

The main goal of this work is to design, implement and evaluate a CAD system for early diagnosis of brain tumor in MR Images. The CAD system is designed and developed utilizing the image processing techniques such as, pre-processing, segmentation, feature extraction and classification.

PROPOSED MULTI-STAGE CAD APPROACH

The proposed approach consists of the following steps

Pre-processing for noise removal and image enhancement, Hybrid enhanced segmentation process for skull removal and tumor region extraction, Feature extraction from the extracted tumor region using statistical texture features and Classification using support vector machine. The proposed system is shown in [Figure-1](#).

In this proposed system, T1-weighted and T2-weighted MR images are considered and given as input to the CAD system. Both the T1-weighted and the T2-weighted MR images are processed separately and combined later for obtaining better results. The T1-weighted MR images are enhanced by sharpening the edges of the image. The T2-weighted MR images are filtered by trilateral filtering where it removes the noise and retains the structural details of the image. Now the processed images of both T1-weighted and T2-weighted are added together to obtain an improved MR image where it is segmented subsequently. In the segmentation process, first the unwanted skull area is removed by applying the skull stripping method. Further, for segregating

the tumor region, an enhanced watershed image segmentation method is applied to the improved MR image. Once the appropriate tumor is extracted, it is classified using support vector machine. The classification method classifies the extracted tumor either as benign or malignant.

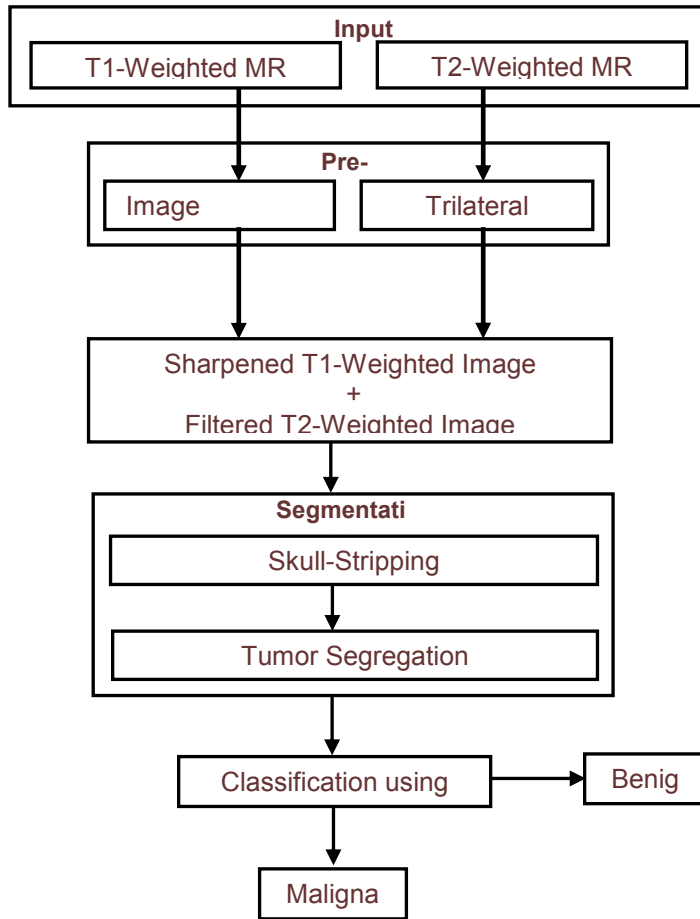


Fig: 1. Overall architecture of the CAD system

MR image pre-processing

The fundamental objective of medical image enhancement is to process the given input image so that the resultant image is more pertinent than the original image for the specific application. The focus of the enhancement is to accentuate or sharpen the image features such as the edges, boundaries or the contrast in order to visualize and for further analysis. The T1-weighted and T2-weighted MR images are considered for the pre-processing procedure. Both the MR images are manipulated and gone through the sharpening and filtering process.

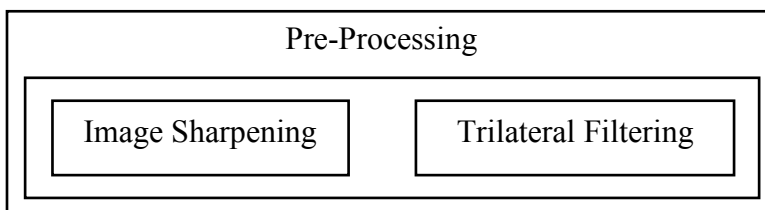


Fig: 2. Pre-processing

Image sharpening

Sharpness describes the clarity of a digital image and the unsharp masks are probably the most common type of sharpening. An unsharp mask cannot generate additional information, but it can significantly improve the edge details. Here, an unsharp mask of the original T1-weighted image is added to the original T1-weighted image to get the sharpened image.

Trilateral filtering

This module has been designed for enhancing the quality of MRI by reducing the noise in the image. Sharp ridges and gutters are commonly found in biomedical images, such as folded gray and white matters in brain MR imaging. Therefore, a narrow spatial window, say, 3 pixels in each dimension, should be used in order to avoid over smoothing structures of sizes comparable to the image resolutions. This leads to the necessity of performing more iterations in the filtering process. In this paper, a trilateral filtering method is used for enhancing the MR images and for noise removal, which works along the same lines as the bilateral filtering. It takes not only the geometric and photometric similarities into account, but also, the local structural similarity to smooth the images with a narrow spatial window while preserving the edges. Local structural information is used to determine inhomogeneity in the images. On one hand, low-pass filtering is performed in the homogeneous regions. On the other hand, smoothing along edges is achieved by considering the geometric, photometric and local structural orientation similarities between neighboring pixels in the inhomogeneous regions. This trilateral approach provides greater noise reduction than bilateral filtering with a 3- pixel-width spatial window. The trilateral filtering is expressed as given in equation (1).

$$MRI^{t+1}(x) = \frac{1}{|Q(x)|} \sum_{t \in Q(x)} MRI^t \cdot w(\xi, x, t) \quad \text{----- (1)}$$

where t is a time variable.

Both T1-weighted and T2-weighted MR images give different levels of contrast. The knowledge about these different contrast levels is exploited for achieving better pre-processing of the given images. The signal in the MRI is murky or bright, depending upon the pulse sequence used and the type of tissue in the image region of interest. The edema and the tumor part is murky in T1-weighted and bright in T2-weighted image. This interesting evidence is well made use of and both T1-weighted and T2-weighted MR images are merged together. The outcome of these combined images yields a favorable result where the image edges are highlighted and the structural information is retained. The obtained result aids in segmenting the image in a superior manner.

Skull stripping for removal of skull

An important procedure in brain image analysis is the skull stripping [10] which involves the removal of the scalp, skull and dura matter. Removal of non-brain tissues, particularly dura, is essential in facilitating accurate measurement of brain structures. Inclusion of non-brain structures can result in mistaken interpretation which makes the detection and analysis very difficult and cumbersome. Another concern in skull stripping is the segregation of non-cerebral and the intracranial tissue due to their homogeneous qualities in their intensities. The process of skull stripping is given below,

- Step 1: Apply local threshold to the trilateral filtered image.
- Step 2: Dilate the threshold image using a structuring element of disc.
- Step 3: Apply masking
- Step 4: Normalize the image for easy extraction of tumor region.

Enhanced watershed segmentation

Watershed segmentation is a predominant segmentation scheme with several advantages. It ensures the closed region boundaries and gives solid results. It is a way of automatically separating or making the regions distinct without touching. The watershed algorithm uses concepts from mathematical morphological operations to partition images into homogeneous regions.

Start

- Step 1: Read the input images, Im_{12} and Im_{22} .
- Step 2: Compute $IM_{12+22}(f) = imfuse(Im_{12}, Im_{22})$
- Step 3: Compute multiscale gradient,
 $MS_{12+22}(f) = \frac{1}{N} \sum_{i=1}^N [Er(Di(IM_{12+22}(f), SE_i) - Er(IM_{12+22}(f), SE_i), SE_{i-1}))]$
- Step 4: Compute $Op_{12} = in_r(\|\nabla f(y(s))\| ds)$
- Step 4: Compute $MS_{Rec_{12+22}}(f) = (MS_{12+22}(f) \oplus SE + Op_{12}, MS_{12+22}(f))$
- Step 5: Create Internal Markers and External Markers.
- Step 6: Apply the created markers to $MS_{Rec_{12+22}}(f)$
- Step 7: Create final Gradient Image, $FG_{12+22}(f)$
- Step 8: Apply watershed $\rightarrow FG_{12+22}(f)$

End

A gradient helps detecting ramp edges and avoids thickening and merging of edges. The local gray level variation in the image can very well be given by the morphological gradient. The gradient image, $G(f)$ is morphologically obtained by subtracting the eroded image, $Er(f)$ from its dilated version, $Di(f)$. The morphological gradient of f is given by

$$G(f) = Di(f) - Er(f) = f \oplus b - f \ominus b \quad \text{----- (2)}$$

where \oplus and \ominus represents the dilation and the erosion respectively.

A multiscale gradient, $IM_{b_{1:n}}(f)$ is the average of morphological gradients of the structuring element, B_i with different scales. The multiscale gradient is given by

$$MS_{b_{1:n}}(f) = \frac{1}{n} \sum_{i=1}^n [Er(Di(IM_{b_{1:n}}(f), SE_i)) - Er(IM_{b_{1:n}}(f), SE_i), SE_{i-1})] \quad \text{----- (3)}$$

where $IM_{b_{1:n}}(f)$ is the fused T1-weighted image and T2-weighted image, SE is the structuring element.

When the computed multiscale gradient is subjected to watershed segmentation process, over-segmentation happens due to the occurrence of trivial minima in the resulting gradient. In order to eliminate this inappropriate minima, the multiscale gradient, $MS_{b_{1:n}}(f)$ is dilated with a structuring element. This structuring element, SE should be smaller than that of the SE that is applied earlier to the multiscale gradient. An optimal threshold, Op_{th} is calculated and added to the dilated $MS_{b_{1:n}}(f)$ to discard the local minima with low contrast.

The optimal threshold value is computed using minimal projection distance. Assume that the image f is an element of the space $K(D)$ of a connected domain D then the topographical distance between points m and n in D is given in equation (4).

$$Op_{th}(m, n) = (m, n) \int \|\nabla f(y(s))\| ds \quad \text{----- (4)}$$

where, m, n is over all paths (smooth curve) inside D , defines the watershed as follows. Let $f \in K(D)$ have a minima, $\{m_i\}_{i \in I}$ for some index set I . The catchment basin $KB(m_i)$ of a minimum m_i is defined as the set of points $K \in D$, which are topographically closer to m_i than to any other regional minimum m_j . The reconstructed gradient image, $MS_{Rec_{b_{1:n}}}(f)$ is obtained by the reconstruction of the multiscale gradient image, $MS_{b_{1:n}}(f)$ with its dilated image.

The internal markers and the external markers are extracted to prevent over-segmentation. Both the markers created are applied to the reconstructed gradient image, $MS_{Rec_{b_{1:n}}}(f)$. Markers are created to identify and distinguish the inner structure of the objects that are to be segmented. Finally, the watershed algorithm [17] is applied to the final gradient image, $FG_{b_{1:n}}(f)$ where a stable and robust object segmentation is obtained.

Feature extraction

Features are extracted from the segmented image using GLCM techniques. Features are the characteristics of the objects of interest. It is the illustrative of the maximum pertinent facts that the image has to offer for a comprehensive characterization of a lesion. Feature extraction methods analyze the various objects in the image and the image itself to extract the most prominent features to classify the objects. The first order image features such as mean, variance, standard deviation, skewness and kurtosis are considered and extracted. Also, the second order image features such as contrast, correlation, energy, homogeneity, smoothness and eccentricity are extracted for this empirical research.

First order features

Mean

Mean is an average value that measures the general illumination of the image. The formula for calculating the mean is given by

$$Int_{mean} = \frac{\sum_{i=1}^{N-1} I(i, j)}{N-1} \quad \text{----- (5)}$$

Variance

The variance is calculated as the average squared deviation of each number from its mean. It tells us how far a set of numbers are spread out from the mean.

$$Int_{var} = \sum_{i=1}^{N-1} \sum_{j=1}^{N-1} (i - \mu)^2 I(i, j) \quad \text{----- (6)}$$

Standard deviation

The standard deviation, σ is a measure that is used to quantify the amount of scattering of a set of pixel values. It is the square root of variance which is given by the formula

$$Int_{sd} = \sqrt{Int_{var}} \quad \text{----- (7)}$$

Skewness

Skewness is defined as a measure of the asymmetry of the probability distribution. It is used to find out whether a wider range of either darker or lighter pixels are present. If the amount of the scattering is intense towards left it is a positive skew. If the amount of the scattering is intense towards right, it is a negative skew.

$$Int_{skew} = \left(\frac{1}{Int_{mean}} \right) \sum_{i=1}^N \sum_{j=1}^N (f(i,j) - Int_{mean})^3 \dots\dots\dots (8)$$

Kurtosis

Kurtosis measures the peak of the probability distribution of a variable. A high kurtosis spreading will have a sharper peak and a flattened tails. A low kurtosis spreading will have a rounded peak with wider shoulder.

$$Int_{kurtosis} = \left(\frac{1}{Int_{mean}} \right) \sum_{i=1}^N \sum_{j=1}^N (f(i,j) - Int_{mean})^4 \dots\dots\dots (9)$$

Second order features

Contrast

Contrast is a measure of intensity juxtapose between a pixel and its neighbouring pixels. Contrast will be 0 for a constant image. It can be calculated by the formula.

$$Tex_{con} = \sum_{i=0}^{N-1} |i - j|^2 P(i,j) \dots\dots\dots (10)$$

Correlation

The gray level linear dependence between the pixels at the specified positions relative to each other is measured by calculating the correlation. Correlation will be +1 or -1 for an accurate positive or negative related image.

$$Tex_{correlation} = \sum_{i=0}^{N-1} \sum_{j=0}^{N-1} \frac{(i \times j) \times P(i,j) - [i] \times [j]}{i \times j} \dots\dots\dots (11)$$

Energy

Energy is also known as uniformity or angular second moment. It returns the sum of squared elements in the gray level co-occurrence matrix. Energy will be 1 for a constant image and is calculated by

$$Tex_{energy} = \sum_{i=0}^{N-1} P(i,j)^2 \dots\dots\dots (12)$$

Homogeneity

Homogeneity returns a value that measures the closeness of the spreading of elements in the GLCM to the GLCM diagonal. The range of the homogeneity ranges from 0 to 1. It is 1 for a diagonal GLCM. Homogeneity can be measured by

$$Tex_{homo} = \sum_{i,j} \frac{P(i,j)}{1+|i-j|} \dots\dots\dots (13)$$

Smoothness

Smoothness measures the relative softness of the intensity in a region. It is defined as

$$Tex_{smooth} = 1 - \frac{1}{1+\sigma^2} \dots\dots\dots (14)$$

Eccentricity

Eccentricity is the ratio of the distance between the centre of the ellipse and its major axis length. The values of eccentricity will be between 0 and 1. An ellipse whose eccentricity is 0, is actually a circle. An ellipse whose eccentricity is 1 will be a line segment. The eccentricity can be measured by

$$Eccentricity = \frac{c}{a} \tag{15}$$

where c is the distance from the centre to the focus of the ellipse and a is the distance from the centre to a vertex

Classification using support vector machine

Classification of the extracted features is performed using Support vector machine (SVM). It is a powerful supervised classifier and an accurate statistical learning theory technique [16] that works on the basis of structural risk minimization principle. The basic purpose of SVM classifier is to choose the appropriate margins between two classes during the training. The kernel in the classifier controls the empirical risk and the categorization competence with the aim of maximizing the margin between the classes and minimize the true costs [1]. In the higher dimension feature space, an optimal separating hyperplane is explored between the members and non-members of the given class. The graphic representation of feature vectors in the input space and in the feature space is represented in Figure- 3.

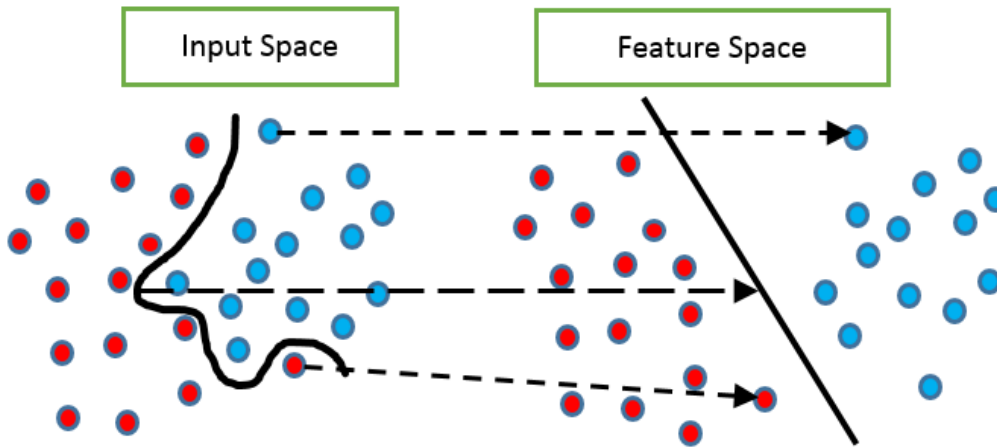


Fig: 3. Representation of feature vectors both in the input space and the feature space

Hyperplane can be defined by H such that

$$x_i \cdot w + b \geq +1 \text{ when } y_i = +1 \tag{16}$$

and

$$x_i \cdot w + b \leq -1 \text{ when } y_i = -1 \tag{17}$$

Here H1 and H2 are termed as two planes and are given by

$$H1: x_i \cdot w + b = +1 \tag{18}$$

$$H2: x_i \cdot w + b = -1 \tag{19}$$

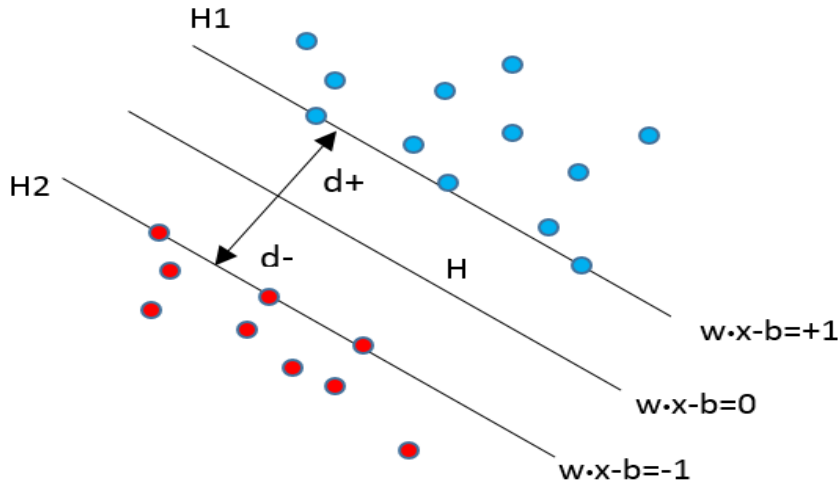


Fig: 4. Selection of the decision boundary between different classes

The points on these planes H1 and H2 are the support vectors. The distance $d+$ is the shortest distance to the closest positive point in the hyperplane. The distance $d-$ is the shortest distance to the closest negative point. The selection of the decision boundary between different classes in the support vector machine is shown in [Figure– 4](#).

The inputs to the SVM algorithm are the gray level co-occurrence matrix (GLCM) features subset extracted from the MR images. The classification procedure separates the input features dataset in the feature space into benign tumors and malignant tumors.

Let us consider that the n -dimensional input x_i ($i = 1, \dots, N$) belong either to the benign class or the malignant class. Let the associated labels be $l_i = +1$ for benign tumor and $l_i = -1$ for malignant tumor. The decision function for the SVM is given by

$$des(x) = w \cdot x + b \text{ ----- (20)}$$

where w is an n -dimensional vector, b is a scalar, and $y_i = des(x_i) \geq 1$ for $i=1, \dots, N$.

A margin is defined as the distance between the separating hyper plane and the training data set nearest to the hyperplane. When the hyperplane decision function, $des(x_i) = 0$ with the maximum margin, an optimal separating hyperplane is achieved.

Quality metrics

Image quality is a basic characteristic of an image that determines the degradation of the observed image compared to a ground truth image. Here, the quality metric parameters such as PSNR, Structural Similarity, Normalized Cross-Correlation and Normalized Absolute Error are computed for its efficiency.

Peak-Signal-to-Noise-Ratio (PSNR)

PSNR is expressed as the ratio between the maximum possible value of a signal and the value of distorting noise that affects the quality of the image. It is inversely proportional to the mean squared error and is measured in decibels. PSNR can be calculated by

$$Met_{psnr} = 10 \log_{10} \frac{(2^8-1)^2}{MSE} \text{ ----- (21)}$$

$$\text{where, } MSE = \frac{1}{MN} \sum_{i=1}^M \sum_{j=1}^N (x(i,j) - y(i,j))^2 \text{ ----- (22)}$$

Here, $x(i,j)$ is the original reference image and $y(i,j)$ is the modified image. i and j are the pixel position of the $M \times N$ image. MSE will be 0 when $x(i,j) = y(i,j)$.

Structural similarity

Structural similarity measures the similarity between two images. It can be measured by the equation

$$Met_{ss} = \frac{\sum_{i,j} \sum_{k,l} (x(i,j) - y(k,l))^2}{\sum_{i,j} \sum_{k,l} (x(i,j))^2} \quad (23)$$

where $x(i,j)$ is the original image and $y(i,j)$ is the modified image.

Normalized cross-correlation (NCC)

NCC measures the similarity between two images. The proximity between these two images can be computed in terms of the correlation function. The NCC is given by the equation

$$Met_{ncc} = \frac{\sum_{i,j} \sum_{k,l} (x(i,j) * y(k,l))}{\sum_{i,j} \sum_{k,l} (x(i,j))^2} \quad (24)$$

Normalized absolute error (NAE)

NAE is the average of absolute difference between the reference image and the modified image. It is calculated by

$$Met_{nae} = \frac{1}{MN} \sum_{i,j} \sum_{k,l} |x(i,j) - y(k,l)| \quad (25)$$

RESULTS AND DISCUSSIONS

Table: 1. Output obtained from various stages of the CAD system


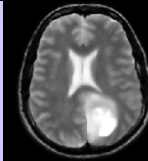
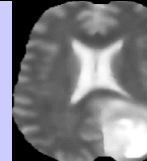
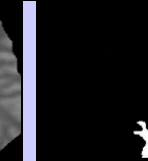
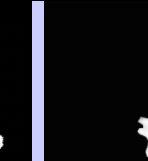
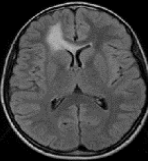
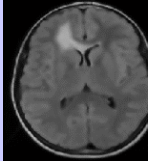
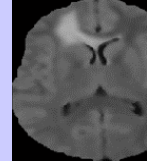
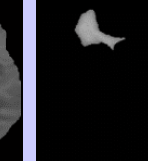
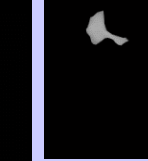
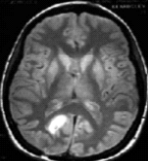
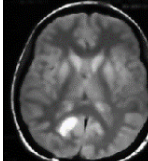
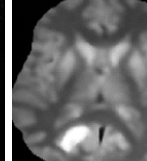
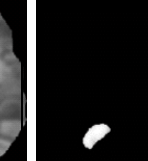
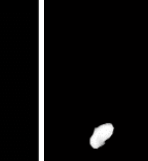
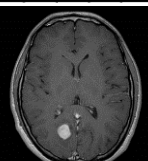
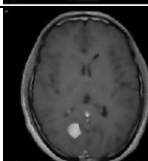
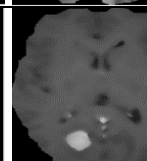
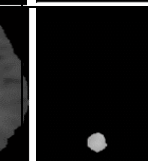
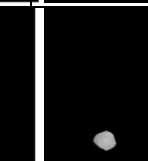
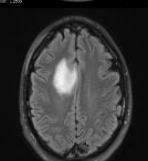
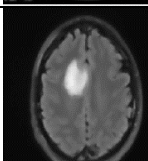
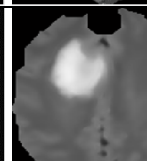
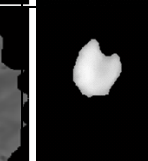
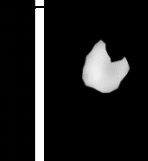
Sl. No	Input Image	Pre-processed Image	Skull Stripped Image	Ground Truth Image	Segmented Image
1					
2					
3					
4					
5					

Table-1 shows five sample image dataset which is processed and manipulated with the developed CAD system. The output obtained in each stage is tabulated in the above table. Only a negligent disparity is observed between the ground truth images and the obtained segmented images which provides higher rate of efficiency.

MRI brain image features and quality assessment

The features of the MR images are of immense importance for better classification. Here, the intensity features and the texture features are extracted effectively from the processed MR images and are tabulated. Moreover, the quality metrics are computed for its efficiency.

GLCM features and quality assessment of the ground truth data

Table: 2. Intensity features obtained from the ground truth images.

Intensity Features					
Image	Mean	Variance	SD	Skewness	Kurtosis
1	0.0227	0.022	0.1491	6.4036	42.0065
2	0.0313	0.0303	0.174	5.3867	30.0162
3	0.0135	0.0133	0.1152	8.4449	72.3164
4	0.012	0.0119	0.1091	8.9484	81.0731
5	0.0723	0.0671	0.259	3.3021	11.9039

Table: 3. Texture features obtained from the ground truth images.

Texture Features						
Images	Contrast	Correlation	Energy	Homogeneity	Smoothness	Eccentricity
1	170.5	0.2335	6.7114	0.0305	0.0217	0.7009
2	170.59	0.4631	4.8804	0.0364	0.0294	0.81
3	128.13	0.6005	0.0011	0.0091	0.0131	0.878
4	122.7	0.0714	0.0013	0.0091	0.0118	0.5186
5	808.63	0.0336	2.1097	0.085	0.0629	0.2811

Table: 4. Quality assessment of the ground truth images using the quality metrics

Quality Assessment				
Images	PSNR	Normalized Cross-Correlation	Structural Content	Normalized Absolute Error
1	17.9215	0.9464	0.992	0.2475
2	27.9011	0.9706	1.0434	0.0981
3	23.3358	0.9543	1.0578	0.1318
4	24.6374	0.9468	1.0567	0.1407
5	25.3106	0.98	0.9972	0.1458

Extracted GLCM features and quality achieved through the CAD system

Table: 5. Intensity features extracted from the input image data

Intensity Features					
Images	Mean	Variance	SD	Skewness	Kurtosis
1	0.0215	0.019	0.1485	6.1932	42.1034
2	0.0311	0.0281	0.169	5.2145	30.1145
3	0.013	0.0132	0.115	8.3023	72.3172
4	0.11	0.0116	0.1089	8.5621	80.9852
5	0.0752	0.0686	0.263	3.4211	12.0121

Table: 6. Texture features extracted from the input image data

Texture Features						
Images	Contrast	Correlation	Energy	Homogeneity	Smoothness	Eccentricity
1	169.8	0.2532	6.5612	0.2991	0.0201	0.8211
2	170.5	0.3932	4.7991	0.0297	0.0281	0.887
3	128.11	0.5908	0.0012	0.009	0.0099	0.898
4	122.2	0.0911	0.0122	0.0089	0.0101	0.5821
5	808.86	0.0412	2.1727	0.09	0.0871	0.2744

Table: 7. Quality metrics computed from the output image

Quality Assessment				
Image	PSNR	Normalized	Structural Content	Normalized Absolute
		Cross-Correlation		Error
1	18.8762	0.9243	0.7712	0.2354
2	25.6754	0.9611	0.9987	0.0972
3	23.4575	0.9367	1.0321	0.1317
4	25.8751	0.9485	0.9989	0.1205
5	27.2136	0.979	0.9811	0.1332

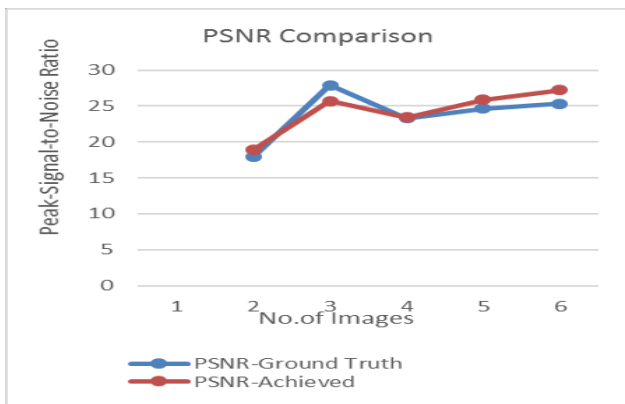


Fig: 5. PSNR: Ground Truth data Vs Achieved data

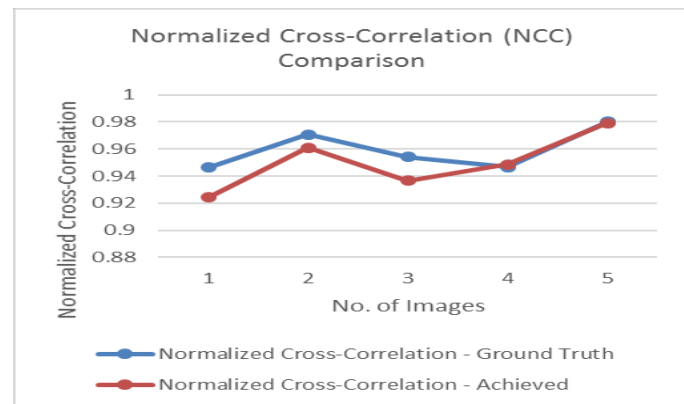


Fig: 6. NCC: Ground Truth data Vs Achieved data

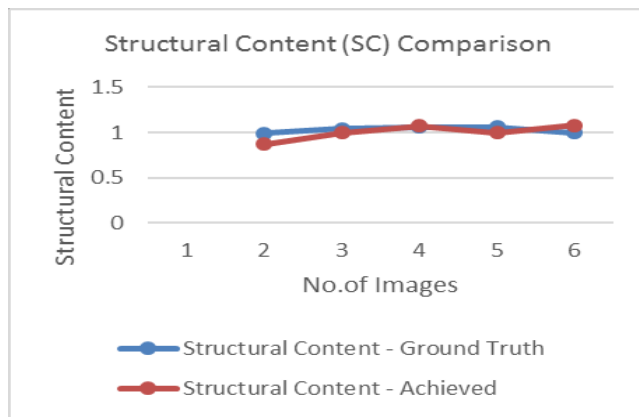


Fig: 7. SC: Ground Truth data Vs Achieved data

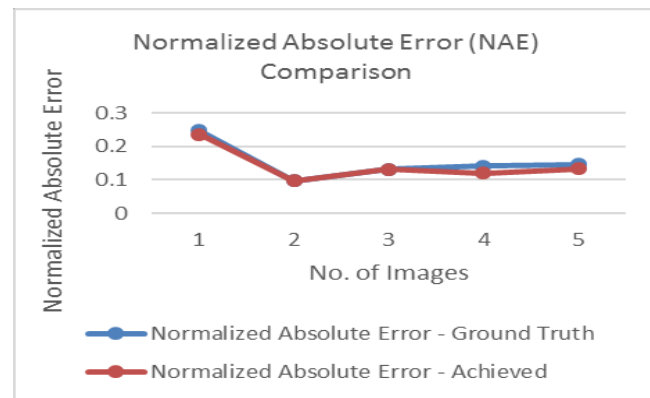


Fig: 8. NAE: Ground Truth data Vs Achieved data

The graphical representation shows the various comparison of the quality metrics for the ground truth image dataset and the actual achieved image dataset. **Figure- 5** shows that the PSNR value is higher for the obtained image compared to the ground truth image data. **Figure- 6** shows that the Normalized Cross-Correlation is lesser compared to the ground truth data. **Figure-7** shows that the structural content is higher in the achieved image data compared to the ground truth image data. And in **Figure- 8**, it is interestingly noted that the Normalized Absolute Error is lesser when compared to the available ground truth MR image data.

Classification

Table: 8. Classification Rates

Methods	TP	TN	FP	FN	Sensitivity (%)	Specificity (%)	Accuracy (%)
Morphology + SVM	20	12	10	8	71	54	64
Watershed + SVM	30	10	5	5	85	66	80
Enhanced Watershed +SVM (Proposed Method)	42	5	2	1	97	71	94

The classification efficiency rates for three different methods are performed and is tabulated in **Table- 8**. It is interesting to observe that the proposed system performed well compared to the other two methods.

Figure-9 depicts the comparative analysis of the three different classification methodologies. The developed CAD system bestows 97 % of sensitivity, 71% of Specificity and were able to achieve 94 % of accuracy.

CONCLUSION

A new and effective computer aided diagnostic (CAD) approach for identifying and classifying the brain tumor is proposed and developed. For this empirical research work, 116 MR images were utilized and employed to yield efficient results. Amongst the 116 MR images, 58 images were T1-weighted and another 58 images were T2-weighted MR images. All the MR images were obtained from Christian Medical College, Vellore, India and Devi Scans, Thiruvananthapuram, India.

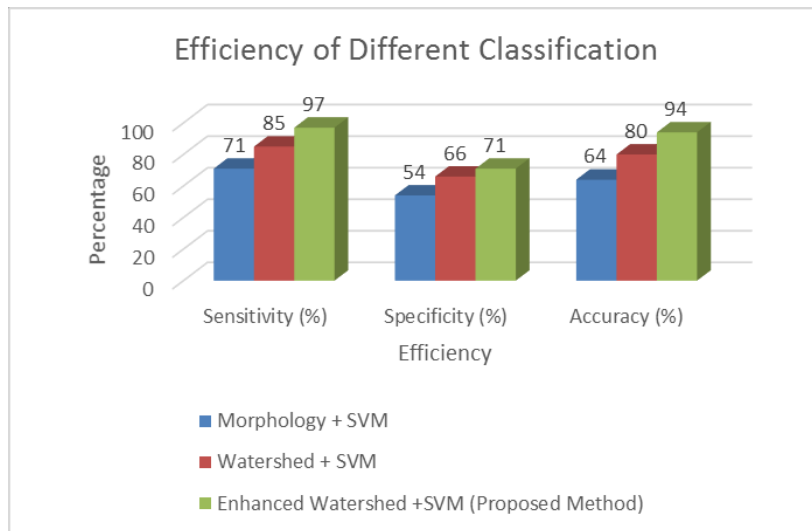


Fig: 9. The efficiency comparison of different classification methods

The developed system is a multi-stage diagnostic system that utilizes the image processing techniques to identify and classify the brain tumor. The proposed system capitalizes with both the T1-weighted and T2-weighted MR images by manipulating and blending it together to obtain an improved results. The enhanced watershed segmentation algorithm is designed and utilized for segmenting the tumor region in the brain effectively. Support vector machine is used to classify the extracted tumor and determine whether the tumor is benign or malignant. The intensity based features and texture based features were extracted by the developed system and is compared to the ground truth dataset. It is interesting to note that the obtained result from the developed system gave better results most of the time when compared to the ground truth dataset. A comparative analysis of two other hybrid classification methods such as Morphology + SVM and Watershed + SVM is performed along with the developed system. By comparing these three classification methods, a higher percentage of efficiency is achieved by the developed system for the brain tumor classification with an accuracy of 94%.

CONFLICT OF INTEREST

Authors declare no conflict of interest.

ACKNOWLEDGEMENT

None.

FINANCIAL DISCLOSURE

Authors have not received any financial support from any individual or organization to carry out this project.

REFERENCES

- [1] International Jin Liu, Min Li, Jianxin Wang, Fangxiang Wu, Tianming Liu, Yi Pan. [2014] A Survey of MRI-Based Brain Tumor Segmentation Methods, *Tsinghua Science and Technology*, 19(6):578–595.
- [2] Muhammed Anshad PY, SS Kumar. [2014] Recent Methods for the Detection of Tumor Using Computer Aided Diagnosis – A Review, International Conference on Control, Instrumentation, Communication and Computational Technologies, *IEEE*, pp: 1014-1019, doi: 978-1-4799-4190-2/14.
- [3] Ramish B. Kawadiwale, Milind E Rane. [2014] Clustering Techniques for Brain Tumor Detection", Proceedings of the Fifth International Conference on Recent Trends in Information, Telecommunication and Computing, *ACEEE*, pp: 299-305, doi: 02.ITC.2014.5.49.
- [4] Akram MU, Usman A. [2011] Computer Aided System for Brain Tumor Detection and Segmentation, 2011 International Conference on Computer Networks and Information

- Technology, *IEEE*, pp:299–302, doi:10.1109/ICC/NIT.2011.6020885.
- [5] Ulku EE, Camurcu AY. [2013] Computer Aided Brain Tumor Detection with Histogram Equalization and Morphological image processing techniques, International Conference on Electronics Computer and Computation, *IEEE*, 48–51.
- [6] Jacek Kawa, Marcin Rudzki, Ewa Pietka, Pawel Szwarc. [2015] Computer Aided Diagnosis Workstation for Brain Tumor Assessment, Proceedings of the 22nd International Conference on Mixed Design of Integrated Circuits and Systems, pp: 98–103.
- [7] SM Ali, Loay Kadom Abood, Rabab Saadoon Abdoon. [2013] Brain Tumor Extraction in MRI images using Clustering and Morphological Operations Techniques, *International Journal of Geographical Information System Applications and Remote Sensing*, 4 (1):1–14.
- [8] P Dvorák, WG Kropatsch, K Bartušek. [2013] Automatic Brain Tumor Detection in T2-weighted Magnetic Resonance Images, *Measurement Science Review*, Technische Universität Wien, 13(5): 223–230.
- [9] Javier Juan-Albarracín, Elies Fuster-García, José V. Manjón, Montserrat Robles, F. Aparici, L. Martí-Bonmatí, Juan M. García-Gómez [2015] Automated Glioblastoma Segmentation Based on a Multiparametric Structured Unsupervised Classification, *PLOS ONE* 10(1):1-20, doi:10.1371/journal.pone.0125143
- [10] D Aju, R Rajkumar. [2015] Locale Detection, Identification and Significant Feature Extraction of brain Tumor Manipulating MR Images, *International Journal of Pharma and Bio Sciences*, 6(4): 291–304.
- [11] SM Ali, Loay Kadom Abood, Rabab Saloon Abdoon. [2014] Automatic Technique to Produce 3D Image for Brain Tumor of MRI Images, *Journal of Babylon University/Pure and Applied Sciences*, 22(7): 1896 – 1907.
- [12] Gaurav R Dandge, Karuna G Bagde. [2014] MRI Brain Images Segmentation & Classification using Texture Features, *International Journal of Computer, Information Technology & Bioinformatics*, 2(1):5–9.
- [13] Chaddad A. [2015] Automated Feature Extraction in Brain Tumor by Magnetic Resonance Imaging Using Gaussian Mixture Models, *Hindawi Publishing Corporation*, 2015: 1–11, dx.doi.org/10.1155/2015/868031.
- [14] Nayak GR, Verma T. [2014] Brain Cancer Classification using Back Propagation Neural Network and Principle Component Analysis, *International Journal of Technical Research and Applications*, 2(4): 26–31.
- [15] Mohammed MR, Reddy ES. [2015] Enhanced Image Fusion Technique for Segmentation of Tumor Using Fuzzy C-Means Cluster Segmentation, *Global Journal of Computer Science and Technology: (F) Graphics & Vision*, Global Journals Inc, 15 (1): 1–4.
- [16] Zhang K., CAO HX, Yan H. [2006] Application of support vector machines on network abnormal intrusion detection, *Application Research of Computers*, 5: 98–100.
- [17] Ali Abdullah Yahya, Jieqing Tan, Min Hu. [2013] A Novel Model of Image Segmentation Based on Watershed Algorithm, *Advances in Multimedia*, Hindawi Publishing Corporation, 1–8.

GUT MICROBIOME OF HONEY BEE - AN INDUSTRIALLY RELEVANT POLLINATOR

Sheik Abduk Kader Sheik Asraf

Department of Biotechnology, Kalasalingam University, Anand Nagar, Krishnankoil – 626 126, Tamil Nadu, INDIA

ABSTRACT

Metagenomics is an important tool to examine the gut microbiota of honey bee [Apis mellifera] – the producer of industrially relevant products such as honey, propolis, royal jelly and wax. Metagenomics approach is useful in analysis of various microbiota factors influencing apiculture: biofilm formation, carbohydrate metabolism, colony collapse disorder, disease progression, horizontal gene exchange, niche adaptation, nutrition. These factors are responsible for increase or decrease in the production of above said industrially relevant products. Causative agents of colony collapse disorder in honey bee namely bacteria, parasites, virus have been identified in the gut through metagenomics. Shotgun and high-throughput are the widely used methods for sequencing of honey bee gut metagenome. Bioinformatics tools, softwares and databases are used for sequence pre-filtering, assembly, identification of microbial diversity, data integration and data analysis of the honey bee gut metagenome. Honey bee gut metagenome serve as biologically relevant marker of colony health. Hygiene, disease resistance, antibiotic resistance, nutrient productions are the key areas governed by the gut microbiota of honey bee. Honey bee gut microbiota act as forerunner for studying gut of higher animals. Honey bee gut is the new paradigm to study the role of beneficial and pathogenic microorganisms.

Received on: 19th-Nov-2015

Revised on: 15th-Nov-2015

Accepted on: 20th-Dec-2015

Published on: 1st-Feb-2016

KEY WORDS

Antibiotic resistance; bioinformatics; colony collapse disorder; honey bee gut; metagenomics

*Corresponding author: Email: ssasraf@gmail.com Tel: 04563 – 289042; Fax: 04563-289322

INTRODUCTION

When Beekeeping industry has gained importance because of two outcomes: direct products [honey, wax, propolis and royal jelly] of the industry and crop pollination of bees. The value of these direct products and pollination service industry is estimated to be around US\$1.2 billion [1] and €22.8-57 billion respectively [2]. This industry is under threat due to Colony Collapse Disorder [CCD]- the sudden loss of worker bees attributed to pathogens [bacteria, parasites and virus], immunodeficiency [due to travel / poor diet], antibiotics, fungicides and pesticides [3, 4]. All these factors affect the normal flora of honeybee gut. In recent times, beekeeping industry has incurred losses worth billions of US\$ worldwide due to CCD [4- 7]. Although, various physical and chemical methods [4, 6] have been put forth to analysis and contain CCD, it proved to be futile.

Metagenomics has emerged as a crucial method in assessment of gut microbiota of healthy as well as CCD honey bees [8, 9]. Shotgun [8] and high-throughput [9] are the widely used methods for sequencing of healthy and CCD honey bee gut metagenomes. Bioinformatics tools, softwares and databases are vital for genome [metagenome in particular] sequencing [10], pre-filtering [11], assembly [12] identification of microbial diversity [10, 11, 13-16], data integration and data analysis [12, 17- 20].

Metagenomics is useful in analysis of diverse microbiota factors influencing apiculture: biofilm formation [9], carbohydrate metabolism [9], colony collapse disorder [21], disease progression [22], horizontal gene exchange [23], niche adaptation [8, 9, 22, 23], nutrition [9, 22, 24]. Causative agents of CCD namely bacteria [25], parasites [21], virus [21] have been identified in the gut of the honey bee through metagenomics. Thus, metagenomics is a significant tool to study the gut of honey bee – the producer of industrially important products and crop pollinator.

HONEY BEE GUT METAGENOME AND METATRANSCRIPTOME ISOLATION

Generally gut microbiota DNA [metagenomic DNA] is used as template for sequencing rather than RNA [metatranscriptome RNA] due to high abundance of rRNA's in the metatranscriptome [26]. CTAB [DNA] and Trizol® [RNA] are the methods used for extractions for respective metagenome and metatranscriptome of honey bee gut [26]. These methods are time consuming and result in less purification factor. However, these methods require lesser monetary resources and the reagents used in these methods can be prepared in bulk for large number of metagenomic samples.

Apart from these conventional methods, a wide variety of kits are available in the market for gut metagenome / metatranscriptome isolation [Table-1]. Most of the honey bee gut metagenomic / metatranscriptome studies [9, 25, 26, 27, 28, 29, 30] utilize Qiagen [Hilden, Germany] manufactured kits [Gentra Puregene Cell Kit, Gentra Puregene Tissue Kit, DNeasy Blood & Tissue Kit, QIAamp DNA Mini Kit, RNeasy Mini Kit]. Other prominent kits utilised for gut metagenomic / metatranscriptome isolation are: UltraClean® Tissue & Cells RNA Isolation Kit, RNA PowerSoil® Total RNA Isolation Kit [31], NucliSENS® easyMAG® [32], RNAqueous®-Micro Total RNA Isolation Kit [33] and FastDNA® SPIN Kit [34] [Table-1].

Gentra Puregene Cell and Gentra Puregene Tissue Kits utilize salting-out precipitation technology to isolate metagenomic DNA from honey bee gut [35, 36]. DNeasy Blood & Tissue kit, QIAamp DNA Mini Kit and RNeasy Mini Kit utilizes Silica technology [37]. Compared to CTAB [DNA] and Trizol® [RNA] methods, these kits provide high quality metagenomic DNA / metatranscriptome in terms of recovery, purification factor and less processing time [35- 37].

BIOINFORMATICS TOOLS, SOFTWARES AND DATABASES - ESSENTIAL FOR HONEY BEE METAGENOMICS

After the isolation, purification and estimation of metagenomic DNA from honey bee gut, the next step is the sequencing. Bioinformatics softwares, tools, on-line programs / resources and databases are highly essential for metagenome sequencing, pre-filtering, assembly, classification of microbial diversity, data incorporation and its analysis [Table-2]. Metagenome sequencing requires robust platforms to complete the task with high accuracy, low cost and greater sequencing reads output. IGA IIX [Illumina Genome Analyzer IIX] and R 454 TS [Roche 454 Titanium Sequencer, Roche Applied Science, Indianapolis, IN] are extensively used sequencing platforms for honeybee gut metagenome sequencing projects [8, 9, 21, 23, 24]. IGA IIX generates reads of length between 35-100 bp. It creates an output of 100 billion bp. [38]. R 454 TS creates ~1,000,000 shotgun Reads per Run and generates reads of length up to 1,000 bp and [8, 9, 22- 24]. It has the utmost consensus precision of about 99.97 % [39]. These two robust sequencing platforms have insured success of honeybee gut metagenome projects.

After the sequencing is completed, pre-filtering of the sequences is essential to sustain the quality of read pairs [9]. Further, the sequences are subjected to a gap-closing examination. RDP-II [40] is the most accepted database for sequence pre-filtering and gap-closing [41]. RDP-II has many applications namely: alignment, annotation, examination and phylogenetically consistent taxonomic support for metagenomic data [40]. Other pipeline includes Pyrotagger [42]. Pyrotagger provides following metagenomic services: filtering of quality reads, trimming of the read span, high proportion of clustering [using pyroclust algorithm], sorting and cataloguing of data [42]. It processes reads of up to 100000 quantities [42].

Assembly of the sequences is the next step. RDP-II [30, 40], Velvet v1.2.10 [43] are used for the assembly of honeybee gut metagenome [9]. Velvet v1.2.10 is a de novo metagenome assembler [44]. It works on the principle of de Bruijn graphs and able to assemble short and longer reads [43, 44].

Annotation of the genes is the key step in the identification of microbial diversity [taxonomic profiling] in the honey bee gut metagenome. MetaPhyler [45], Integrated Microbial Genomes /Metagenome Expert Review [IMG/MER] [46] are used for annotation of assembled honeybee gut metagenome with the availability of metagenome datasets. MetaPhyler [45] uses phylogenetically linked marker genes for taxonomic cataloguing of metagenomic reads. It works on the principle of BLAST. MetaPhyler is considered to be superior compared to its predecessors [PhymmBL, MEGAN] [47]. IMG/MER [46] has numerous tools for analysis [IMG/M UI Map] that provides the

users [with private password] for thorough assessment and modification of the honey bee gut metagenome sample[s]' annotations [48].

Geneious Pro v5.6 [49] is used for honeybee gut metagenome data integration. It has various applications: metagenome browsing, phylogenetic tree construction, metagenome grouping visualization [50]. It can handle data from wide variety of sequencing platforms: Sanger, NGS, barcoded. It works on almost in all computer platforms: Windows, Mac and Linux [50].

IMG/MER [46], MEGAN [47], MOTHUR [30, 51] are used for honeybee gut metagenome data analysis. MEGAN performs taxonomic study, efficient examination using following classifications: COG/NOG, KOG, KEGG, SEED [52]. It is used for relative visualization, rarefaction analysis, principal coordinate analysis and clustering of metagenome data [52]. It also provides various charts and plots: space-filling radial trees, wordclouds, bubble charts, co-occurrence plot [52]. Metadata specifying and viewing of metagenome samples as rared/shared/core/total biomes is possible with the use of MEGAN [53]. MOTHUR [30, 51] analyzes honey bee gut metagenome data generated by wide range of sequencing platforms namely: Illumina [HiSeq/MiSeq], IonTorrent, Sanger and 454 [54].

NCBI, ARB-SILVA, Greengenes and RDP databases [55] serve as vital repository for honey bee gut metagenomes. In NCBI, there are at present 3 BioProjects related to honey bee gut metagenomes [1, 56]. SILVA is a database of ARB software package [57]. ARB has a graphic, integrated environment of software tools for receiving and analysis of honey bee gut metagenome sequence information [57]. Greengenes is used for browsing, exporting, comparing, searching, aligning, trimming of honey bee gut metagenome data [58].

MICROBIOTA OF HONEY BEE IDENTIFIED BY METAGENOMICS

After performing metagenome sequencing, pre-filtering, assembly, identification of microbial diversity, “data integration and its analysis” is the key to unlock the potential of the microbiota of honey bee gut. Gilliamella and Snodgrassella [Table–3] are found to be predominantly present [59] in all the honey bee gut metagenomes: Gilliamella apicola [9, 8, 29], Gilliamella sp. [9], G. apicola wkB1T [23], Snodgrassella alvi [8,9], Snodgrassella sp. [9], S. alvi wkB2T [23]. Both, G. apicola and S. alvi are present only in pH neutral hive niches [60]. G. apicola and S. alvi showed high percentage of 16S rRNA similarity and multiple strains are present in the same gut sample [59] because of their frequent recombination. Both, phylogenies of G. apicola and S. alvi show major similarity with the phylogenies of their hosts [29]. G. apicola is present generally in the midgut and hindgut regions [60]. Moreover, significant numbers of recombination events occur in Gilliamella sp when compared to S. alvi [61, 62]. One phylotype within Betaproteobacteria [“Candidatus S. alvi”], and one within Gammaproteobacteria [“Candidatus G. apicola”] are present in each and every one of the gut metagenomes suggesting the importance of Snodgrassella and Gilliamella [61].

Actinobacteria, γ -Proteobacteria [Frischella perrara] and Bacilli, the core group of bacteria responsible for breakdown of polysaccharides, fermentation and production of honey [24, 63] have been identified by metagenomics. A key family namely Acetobacteraceae responsible for microbial persistence in larval stage is present in first and second larval instars[22]. γ -proteobacterial species [having genes encoding pectin-degrading enzymes] responsible for breakdown of pollen walls and honey formation [9] have been identified by metagenomics. Bifidobacterium sp. [31, 34], Lactobacillus kunkeei [60], Acetobacteraceae and Lactobacillus sp., the probiotics species are present in honey bee gut [9]. Bifidobacterium sp. provides defensive mechanism to honey bee to ward off potential pathogens [31]. L. kunkeei controls the larval gut and beebread, the key niches of honey bee [22]. These species are responsible for maintaining the probiotic nature of the gut.

CCD as described earlier is responsible for loss of billions of US\$ to the beekeeping industries in the continents of Americas [4, 6], Europe [5], and Africa [7]. Indiscriminate use of pesticides, antibiotics in beekeeping industries has led to development of pesticide and antibiotic resistance in the worker honeybees [3]. All these factors affect the normal flora of honeybee gut leading to the large scale collapse of honeybee colonies [2, 21]. Metagenomics unlike erstwhile physical and chemical methods has able to recognize and differentiate the normal gut microbiota and causative agents [bacteria, parasites and virus] of CCD. Metagenomics analysis has prevented further loss of worker bees due to CCD.

Pathogenic bacteria, fungi, parasite, virus to blame for loss of honey bee colonies have been identified by metagenomics. Principal pathogens include Burkholderia [25], Wolbachia, Mucor hiemalis, Nosema apis, N.

ceranae [64], Crithidia [65], Lake Sinai virus [LSV] [27, 33], black queen cell virus [BQCV], acute bee paralysis virus [ABPV], deformed wing virus [DWV] [28], Israeli acute paralysis virus [IAPV] [27], Kashmir bee virus [KBV] and sacbrood virus [SV] [21]. Wolbachia is a persistent honey bee associate. Among these pathogens Israeli acute paralysis virus is found to be highly contagious [21]. Burkholderia [25] is found in lone individual bees. *M. hiemalis* kills honey bees under various conditions [21]. Nosema species [*N. apis*, *N. ceranae*] is very much prevalent [21] in honey bees [100% in case of CCD]. *N. ceranae* works in synergistic with the wide variety of virus: BQCV, ABPV, DWV, KBV [33] to cause CCD.

Through gut metagenomics, an 18S rRNA gene of about ~700 nucleotide section is identified to be of the parasite Crithidia [21]. Crithidia is controlled in gut by the presence of Gilliamella [65]. New strains of LSV [27,33] have emerged in recent times in both USA and Europe. ABPV and KBV are closely related virus responsible for CCD [33] and KBV in particular is prevalent in CCD colonies in major parts of USA [33]. DWV is responsible for loss of colonies during fall season in USA [5]. Recently, a new variant of IAPV has been identified [27]. Through metagenomics approach, it is proved that Iridovirus does not cause CCD [32].

Antibiotic resistance poses severe threat for survival of honey bee colonies. Tetracycline resistance is a leading cause for loss of colonies [66]. Through metagenomics approach, 8 tetracycline resistance loci namely: genes coding for efflux pump and genes coding for ribosome protection are identified from microbiota associated with tetracycline exposed bee colonies [66].

GUT MICROBIOTA FACTORS INFLUENCING APICULTURE: IDENTIFIED BY METAGENOMICS

Microbiota factors are responsible for the increase in the yield of apiculture products [67]. Various metagenomics sequencing methods have been employed to study these factors [Table-3]. Biofilm formation by the gut microbiota is responsible for pathogen defense, thereby preventing the loss of worker bees against protozoan parasite [9]. Carbohydrate metabolism by gut microbiota results in efficient nutrient utilization leading to increase in honey production [9, 22, 24]. Disease progression and resistance is influenced by gut microbiota, thereby maintaining the general health honeybee colony [22]. Horizontal gene exchange among gut symbionts is responsible for the host specificity [23].

Niche adaptation is a critical factor for diversification of gut microbiota among different species of honey bee. This factor is responsible for breakdown of pollen walls for nutrition, energy metabolism, microbial succession [8, 9, 22, 23].

FUTURE DIRECTIONS OF HONEY BEE GUT METAGENOMICS

Future research in honey bee gut metagenomics depends upon the information generated through the sequencing projects. Further, a fully dedicated database would serve as a repository of data generated and further relevant information would be obtained. Using this information, new drug targets can be developed to counter the menace of CCD. This would result in enhancement of life span of honey bees resulting increased pollination and production of honey, propolis, royal jelly and wax.

CONCLUSION

Honey bee gut metagenome serve as indicator of its health [34] and a marked change in the metagenome composition can be used as biological marker of the colony health [25, 27, 33]. Broad-spectrum hygiene, disease prevention, synthesis of nutrients in the honey bee colonies is due to the core beneficial microbial community present in the gut metagenome [24, 31, 60]. Well-organized evolutionary aspects of honey bee gut microbiota serve as model to study gut microbiota of higher animals [8]. CCD and antibiotic resistance is comprehensively studied using metagenomics [3, 32, 66]. Metagenomics has revealed that vertical transmission of gut microbiota from mother to daughter honey bees and also role of worker bees [29, 63]. Thus, honey bee emerged as front runner in the study of gut metagenomics in particular to that of beneficial bacteria [9, 23, 30, 55].

Table: 1. Honey bee gut metagenome DNA/RNA isolation Kits

Kit	Manufacturers	References
FastDNA® SPIN Kit	MP Biomedicals [India] Pvt Ltd, Mumbai, India	34
RNAqueous®-Micro Total RNA Isolation Kit	Invitrogen BioServices India Pvt. Ltd, Bangalore, India	33
Gentra Puregene Cell Kit	Qiagen, Hilden, Germany	9
DNeasy Blood & Tissue Kit	Qiagen, Hilden, Germany	26
QIAamp DNA Mini Kit	Qiagen, Hilden, Germany	27
RNeasy Mini Kit	Qiagen, Hilden, Germany	28
Gentra Puregene Tissue Kit	Qiagen, Hilden, Germany	25
UltraClean® Tissue & Cells RNA Isolation Kit	MO BIO Laboratories, Inc, Carlsbad, USA	31
NucliSENS® easyMAG®	bioMerieux, Inc, Durham, USA	32

Table: 2. Bioinformatics tools, softwares and databases used in honey bee gut metagenomics

Databases, Platforms, Softwares, Tools	References	
Pre-filtering and gap-closing	RDP-II	40
	Pyrotagger	42
Assembly of the sequences	RDP-II	40
	Velvet v1.2.10	43
Annotation of the genes	MetaPhyler	45
	IMG/M ER	46
Data integration	Geneious Pro v5.6	49
Data analysis	IMG/M ER	46

Table: 3. Factors influencing apiculture identified by etagenomics

Factors	Microbiome	Sequencer
Biofilm formation	G. apicola S. alvi	IGA IIX*
Carbohydrate metabolism	Gilliamella sp. Snodgrassella sp.	IGA IIX*
	γ-Proteobacteria, Bacilli	IGA IIX*
Horizontal gene exchange	G. apicola wkB1T S. alvi wkB2T	IGA IIX*
Niche adaptation	Gilliamella sp. Snodgrassella sp.	IGA IIX*
	G. apicola S. alvi	IGA IIX*
	G. apicola wkB1T S. alvi wkB2T	IGA IIX*

IGA IIX* - Illumina Genome Analyzer IIX;

CONFLICT OF INTEREST

There is no conflict of interest.

ACKNOWLEDGEMENT

The author thanks all the authors listed in the references for providing the reprints.

FINANCIAL DISCLOSURE

No financial support was received for this study.

REFERENCES

- [1] <http://www.ncbi.nlm.nih.gov/bioproject/52851> [accessed 21 November 2014]
- [2] Kluser S et al.[2011] UNEP emerging issues: global honey bee colony disorder and other threats to insect pollinators. Geneva: United Nations Environment Programme.
- [3] Evans JD et al.[2009] Colony collapse disorder: a descriptive study. *PloS One*
- [4] Johnson R [2010] Honey bee colony collapse disorder. *Washington: Congressional Research Service* 7–5700.
- [5] Dainat B et al.[2012] Colony collapse disorder in Europe. *Environmental microbiology reports* 4:123–125.
- [6] Stankus T. [2008] A review and bibliography of the literature of honey bee Colony Collapse Disorder: a poorly understood epidemic that clearly threatens the successful pollination of billions of dollars of crops in America. *Journal of Agricultural & Food Information* 9:115–143.
- [7] Torto B. [2011] Colony collapse disorder: myth or reality in Africa?. 107th COLOSS Conference - Belgrade, SERBIA, 26-28 August, 2011
- [8] Engel P, Moran NA. [2013] Functional and evolutionary insights into the simple yet specific gut microbiota of the honey bee from metagenomic analysis. *Gut Microbes* 4:60–65.
- [9] Engel P et al.[2012] Functional diversity within the simple gut microbiota of the honey bee. *Proceedings of the National Academy of Sciences* 109:11002–11007.
- [10] Dinakaran V et al.[2014] Elevated Levels of Circulating DNA in Cardiovascular Disease Patients: Metagenomic Profiling of Microbiome in the Circulation. *PloS One*
- [11] Rajendhran J, Gunasekaran P. [2011] Microbial phylogeny and diversity: small subunit ribosomal RNA sequence analysis and beyond. *Microbiological research* 166:99–110.
- [12] Asraf SS et al.[2012] Genomics Perspectives of Bioethanol Producing *Zymomonas mobilis*. In *Global Sustainable Development and Renewable Energy Systems* Ed. Olla, P. IGI Global, Hershey, PA, USA. 209–233
- [13] Krishnan M et al.[2014] Insect gut microbiome - An unexploited reserve for biotechnological application. *Asian Pacific journal of tropical biomedicine* 4[Suppl 1]: S16–S21.
- [14] Rajendhran J, Gunasekaran P. [2008] Strategies for accessing soil metagenome for desired applications. *Biotechnology advances* 26:576–590
- [15] Rajesh T et al.[2012] Genomic Technologies in Environmental Bioremediation. In *Microorganisms in Environmental Management, Springer Netherlands* 701–718.
- [16] Rajesh T et al.[2013] Analysis of Microbial Diversity and Construction of Metagenomic Library. In *Analyzing Microbes Springer Berlin Heidelberg* 187–208.
- [17] Asraf SS et al.[2009] Functional genomic analysis of putative ORF ZMO0904 of *Zymomonas mobilis* ZM4. The 11th International Conference on Molecular Systems Biology, Shanghai, China. June 21–25, 2009. 96.
- [18] Asraf SS et al.[2011] Bioinformatics and biosynthesis analysis of cellulose synthase operon in *Zymomonas mobilis* ZM4. *Journal of Institute of Integrative Omics and Applied Biotechnology* 2:1–7.
- [19] Asraf SS et al.[2013] Computational and functional analysis of β -lactam resistance in *Zymomonas mobilis*. *Biologia* 68:1054–1067
- [20] Rajnish KN et al.[2011] Functional characterization of a putative β -lactamase gene in the genome of *Zymomonas mobilis*. *Biotechnology letters* 33:2425–2430.
- [21] Cox-Foster DL et al.[2007] A metagenomic survey of microbes in honey bee colony collapse disorder. *Science* 318.5848:283–287.
- [22] Vojvodic S et al.[2013] Microbial Gut diversity of Africanized and European honey Bee larval instars. *PLoS one*
- [23] Kwong WK et al.[2014] Genomics and host specialization of honey bee and bumble bee gut symbionts. *Proceedings of the National Academy of Sciences* 111:11509–11514.
- [24] Lee FJ et al.[2014] Saccharide breakdown and fermentation by the honey bee gut microbiome. *Environmental Microbiology* doi: 10.1111/1462-2920.12526. [Epub ahead of print].
- [25] Martinson VG et al.[2011] A simple and distinctive microbiota associated with honey bees and bumble bees. *Molecular Ecology* 20:619–628.
- [26] Evans J D et al.[2013] Standard methods for molecular research in *Apis mellifera*. *Journal of Apicultural Research* 52:1–54.
- [27] Granberg F et al.[2013] Metagenomic detection of viral pathogens in spanish honeybees: co-infection by aphid lethal paralysis, Israel acute paralysis and lake sinai viruses. *PLoS One*
- [28] Johnson RM et al.[2009] Changes in transcript abundance relating to colony collapse disorder in honey bees [*Apis mellifera*]. *Proc Nat Acad Sci USA* 106:14790–14795.
- [29] Koch H et al.[2013] Diversity and evolutionary patterns of bacterial gut associates of corbiculate bees. *Mol Ecol* 22:2028–2044.
- [30] Martinson VG et al.[2012] Establishment of characteristic gut bacteria during development of the honeybee worker. *Applied and environmental microbiology* 78:2830–2840
- [31] Mattila HR et al.[2012] Characterization of the active microbiotas associated with honey bees reveals healthier and broader communities when colonies are genetically diverse. *PLoS One*
- [32] Tokarz R, Firth et al.[2011] Lack of evidence for an association between Iridovirus and colony collapse disorder. *PLoS One* .
- [33] Cornman RS et al.[2012] Pathogen webs in collapsing honey bee colonies. *PLoS One*
- [34] Ahn JH et al.[2012] Pyrosequencing analysis of the bacterial communities in the guts of honey bees *Apis cerana* and *Apis mellifera* in Korea. *J Microbiol* 50:735–745.
- [35] <http://www.qiagen.com/in/products/catalog/sample-technologies/dna-sample-technologies/genomic-dna/genra->

- puregene-cell-kit/#technical specification [accessed 19 November 2014]
- [36] http://www.qiagen.com/in/products/catalog/sample-technologies/dna-sample-technologies/genomic-dna/genra-puregene-tissue-kit/#technical_specification [accessed 19 November 2014]
- [37] http://www.qiagen.com/in/products/catalog/sample-technologies/dna-sample-technologies/genomic-dna/qiaamp-dna-mini-kit/#technicalspe_cification [accessed 19 November 2014]
- [38] http://res.illumina.com/documents/products/datasheets/datasheet_genome_analyzeriix.pdf [accessed 6 November 2014]
- [39] <http://454.com/products/gs-flx-system/> [accessed 1 November 2014]
- [40] Cole JR et al.[2007] The ribosomal database project [RDP-II]: introducing myRDP space and quality controlled public data. *Nucleic acids research* 35[suppl 1]:D169–D172.
- [41] <http://rdp.cme.msu.edu/misc/about.jsp> [accessed 4 November 2014]
- [42] Kunin V, Hugenholtz P. [2010] Pyrotagger: A fast, accurate pipeline for analysis of rRNA amplicon pyrosequence data. *The Open Journal* [Article1]:1–8.
- [43] Zerbino DR, Birney E. [2008] Velvet: algorithms for de novo short read assembly using de Bruijn graphs. *Genome research* 18:821–829.
- [44] <https://www.ebi.ac.uk/~zerbino/velvet/> [accessed 1 November 2014]
- [45] Liu B et al.[2010], December] MetaPhyler: Taxonomic profiling for metagenomic sequences. In *Bioinformatics and Biomedicine [BIBM]*, 2010 IEEE International Conference, *IEEE*. 95–100
- [46] Markowitz VM et al.[2009] IMG ER: a system for microbial genome annotation expert review and curation. *Bioinformatics* 25:2271–2278
- [47] <http://metaphyler.cbcb.umd.edu/> [accessed 3 November 2014]
- [48] <http://img.jgi.doe.gov/> [accessed 1 November 2014]
- [49] Drummond A et al.[2012]. Geneious v5. 6. Created by Biomatters. <http://www.geneious.com>.
- [50] <http://www.geneious.com/> [accessed 5 November 2014]
- [51] Schloss PD et al.[2009] Introducing mothur: open-source, platform-independent, community-supported software for describing and comparing microbial communities. *Applied and environmental microbiology* 75:7537–7541.
- [52] <http://ab.inf.uni-tuebingen.de/software/megan5/> [accessed 8 November 2014]
- [53] Huson DH et al.[2007] MEGAN analysis of metagenomic data. *Genome research* 17:377–386.
- [54] <http://www.mothur.org/> [accessed 10 November 2014]
- [55] Newton IL, Roeselers G [2012] The effect of training set on the classification of honey bee gut microbiota using the Naïve Bayesian Classifier. *BMC Microbiol* 12:1–9.
- [56] <http://www.ncbi.nlm.nih.gov/bioproject/82567> [accessed 21 November 2014]
- [57] <http://www.arb-silva.de/> [accessed 15 November 2014]
- [58] <http://greengenes.lbl.gov/cgi-bin/nph-index.cgi> [accessed 17 November 2014]
- [59] Engel P et al.[2014] Hidden Diversity in Honey Bee Gut Symbionts Detected by Single-Cell Genomics. *PLoS genetics*
- [60] Anderson KE et al.[2013] Microbial ecology of the hive and pollination landscape: bacterial associates from floral nectar, the alimentary tract and stored food of honey bees [*Apis mellifera*]. *PLoS One*.
- [61] Moran NA et al.[2012] Distinctive gut microbiota of honey bees assessed using deep sampling from individual worker bees. *PLoS One* .
- [62] Sabree ZL et al.[2012] Independent studies using deep sequencing resolve the same set of core bacterial species dominating gut communities of honey bees. *PLoS One*
- [63] Powell JE et al.[2014] Routes of Acquisition of the Gut Microbiota of the Honey Bee *Apis mellifera*. *Applied and environmental microbiology* 80:7378–7387.
- [64] Chen YP et al.[2009] Morphological, Molecular, and Phylogenetic Characterization of *Nosema ceranae*, a Microsporidian Parasite Isolated from the European Honey Bee, *Apis mellifera*. *Journal of eukaryotic microbiology* 56:142–147.
- [65] Cariveau DP et al.[2014] Variation in gut microbial communities and its association with pathogen infection in wild bumble bees [*Bombus*]. *The ISME journal* 8:2369–2379.
- [66] Tian B et al.[2012] Long-term exposure to antibiotics has caused accumulation of resistance determinants in the gut microbiota of honeybees. *mBio* 3:e00377-12 <http://dx.doi.org/10.1128/mBio.00377-12>.
- [67] http://www.fintrac.com/cpanelx_pu/Ethiopia%20CIAFS/12_06_4_949_CIAFS%20_1%20Honey%20Final%20Oct%2011.pdf, [accessed 31 March 2014]

ISOLATION AND CHARACTERIZATION OF A MOLYBDENUM-REDUCING AND AMIDE-DEGRADING *BURKHOLDERIA* SP. STRAIN NENI-11 IN SOILS FROM WEST SUMATERA, INDONESIA

Rusnam Mansur^{1*}, Neni Gusmanizar^{2,3}, Farrah Aini Dahalan⁴, Noor Azlina Masdor⁵, Siti Aqlima Ahmad², Mohd. Shukri Shukor⁶, Muhamad Akhmal Hakim Roslan², Mohd. Yunus Shukor²

¹Dept of Agricultural Engineering, Faculty of Agricultural Technology, Andalas University, Padang, 25163, INDONESIA

²Dept of Biochemistry, Faculty of Biotechnology and Biomolecular Sciences, Universiti Putra Malaysia, UPM 43400 Serdang, Selangor, MALAYSIA

³Dept of Animal Nutrition, Faculty of Animal Science, Andalas University, Padang, 25163, INDONESIA

⁴School of Environmental Engineering, Kompleks Pusat Pengajian Jejawi 3, Universiti Malaysia Perlis, 02600 Arau, Perlis, MALAYSIA

⁵Biotechnology Research Centre, MARDI, P. O. Box 12301, 50774 Kuala Lumpur, MALAYSIA

⁶Snoc International Sdn Bhd, Lot 343, Jalan 7/16 Kawasan Perindustrian Nilai 7, Inland Port, 71800, Negeri Sembilan, MALAYSIA

ABSTRACT

A molybdenum-reducing bacterium isolated from contaminated soil was able to utilize acrylamide as the electron donor source, and was able utilize acrylamide, acetamide and propionamide for growth. Reduction was optimal at pH between 6.0 to 6.3, at temperatures of between 30 and 37 °C, glucose as the electron donor, phosphate at 5.0 mM, and sodium molybdate at 15 mM. The absorption spectrum of the Mo-blue indicates it is a reduced phosphomolybdate. Molybdenum reduction was inhibited by mercury (ii), silver (i) and chromium (vi) at 2 p.p.m. by 91.9, 82.7 and 17.4 %, respectively. Biochemical analysis resulted in a tentative identification of the bacterium as *Burkholderia cepacia* strain Neni-11. The growth of this bacterium modelled according to the modified Gompertz model. The growth parameters obtained were maximum specific growth rates of 1.241 d⁻¹, 0.971 d⁻¹, 0.85 d⁻¹ for acrylamide, propionamide and acetamide, respectively, while the lag periods of 1.372 d, 1.562 and 1.639 d were observed for acrylamide, propionamide and acetamide, respectively. The ability of this bacterium to detoxify molybdenum and grown on toxic amides makes this bacterium an important tool for bioremediation.

Received on: 12th-Oct-2015

Revised on: 14th-Jan-2016

Accepted on: 15th-Jan-2016

Published on: 8th-March-2016

KEY WORDS

Molybdenum reduction;
molybdenum blue; *Burkholderia*
sp.; acrylamide;
propionamide;
acetamide

*Corresponding author: Email: rusnam_ms@yahoo.com Tel: +62081374974481; Fax: +620751-777413

INTRODUCTION

Mining activities are the major source of molybdenum pollution. In Indonesia, copper and gold mining activity from the copper-gold-molybdenum porphyry deposit in Batu Hijau, Sumbawa has steadily contaminated surrounding coastal regions. The mine deposits nearly several million tonnes of waste tailings to the sea annually. This has led to decreased fish population and water quality [1,2]. A similar situation is seen in a molybdenum mine in western Liaoning China, where the molybdenum mine tailings have polluted the Nver River. The river water and sediment contain molybdenum at levels far exceeding the statutory limits [3]. In Armenia, numerous copper-molybdenum mines and a copper-molybdenum metallurgical plant in Alaverdi, the latter operating without a proper filtration system since 1996 have polluted nearly 300 square kilometres of land [4]. In the Miduk Copper Complex in Iran, in which molybdenum is a valuable by-product, the complex tailings dam has triggered a high concentration of molybdenum found in the borehole near a drinking water source. Metal seepage and infiltration towards the surrounding surface and groundwater from the metal tailings dam is frequently inevitable, causing the observed pollution [5]. In Malaysia, the Mamut copper mine in Ranau Sabah, produced gold and molybdenum as

by-products. Episodic ruptures of the pipes carrying metal-rich wastes have caused the contamination of the surrounding agricultural areas and the Ranau River [6,7].

Substantial nutritional consumption of molybdenum brings about a secondary copper deficit. The symptoms, mainly documented in ruminants are observed globally. Cattle and sheep are ten times more prone compared to non-ruminants. The sulfur-rich conditions in the rumen favour formation of thiomolybdate compounds. As these compounds chelate copper, the bioavailability of copper diminished and copper deficiency symptoms such as weight loss, anemia, diarrhea kidney damage, and osteoporosis occur [8]. Spermatogenesis in several organisms is also negatively affected by molybdenum. Molybdenum supplementation in the fruit fly *Drosophila* severely disturbed spermatogenesis [9]. Rats are also affected. Molybdenum (ammonium molybdate) supplementation to the adult male Wistar rats diet leads to histopathological and histomorphometric with a substantial weight reduction of the testes [10]. Spermatogenesis in the testicular organ culture of the Japanese eel induced by the compound 11-ketotestosterone (11KT) is also inhibited by a combination of heavy metals including molybdenum. A synergistic effect of molybdenum was observed in this study [11].

Aside from heavy metals, organic pollutants or manmade chemicals (xenobiotics) such as phenol, acrylamide, nicotinamide, acetamide, iodoacetamide, propionamide, acetamide, sodium dodecyl sulfate (SDS) and diesel are major global pollutants [12–14]. Amides such as acrylamide, acetamide and propionamide are produced in the order of millions of tonnes per year [15]. Acrylamide is chiefly used to synthesize the polymer polyacrylamides [16]. Acetamide is used as a plasticizer and as an industrial solvent while propionamide is used as an ingredient in many different organic processes to form other useful compounds. Amongst these amides, acrylamide is very toxic. The acrylonitrile-acrylamide industries are known sources acrylamide pollution with levels as high as 1 g/L have been reported [17]. Another non-documented source of acrylamide comes from glyphosate application in agriculture areas. The formulation of this pesticide uses 20-30% polyacrylamide as a dispersing agent [18], and this could be a substantial source of acrylamide pollution in soils and run-offs.

Removal of soluble molybdenum through bacterial reduction is a promising bioremediation strategy [19]. In bacterial reduction of molybdenum to the colloidal molybdenum blue, the Mo-blue aggregates with bacterial biomass can aid in its removal [20]. Since it was first discovered in 1896, [21] many more Mo-reducing bacteria have been isolated [19, 22, 23]. Some microbes are able to degrade a variety of xenobiotics including acrylamide [24] and detoxify heavy metals at the same time including the reduction of chromate coupled with the biodegradation of phenol [25].

In this work, we successfully isolated a novel molybdenum reducing bacterium showing the capacity to grow on various amide and nitrile compounds. The novel characteristics of this bacterium will make the bacterium suitable for the bioremediation of polluted sites having these pollutants in the future.

MATERIALS AND METHODS

Molybdenum-reducing bacterium growth and maintenance

Soil samples were taken (5 cm deep from topsoil) from the grounds of a garbage-contaminated land in the province of Pariaman, Sumatera, Indonesia in January 2009. Isolation of molybdenum-reducing bacteria utilized a minimal salts media (MSM) with the phosphate concentration set at 5 mM. The MSM was also supplemented with sodium molybdate at 10 mM. Preparation of soil bacterial suspension was carried out by adding soil (1.0 gram) to 10 ml of deionized water. The soil suspension was thoroughly mixed, and 0.1 mL of the soil suspension was then spread onto a petri dish containing agar of a media (w/v) as follows: yeast extract (0.5%), $MgSO_4 \cdot 7H_2O$ (0.05%), $Na_2MoO_4 \cdot 2H_2O$ (0.242 % or 10 mM), glucose (1%), $(NH_4)_2SO_4$ (0.3%), NaCl (0.5%), agar (1.5%), and Na_2HPO_4 (0.071% or 5 mM). The pH of the media was adjusted to pH 6.5 [23]. This media is known as a low phosphate molybdate media or LPM. After 48 hours of incubation at room temperature, several white and ten blue colonies appeared on the plate. The ten isolates were then restreaked on the LPM agar several times in order to get pure culture. Mo-blue production from these bacteria was then quantified in 100 mL liquid culture (LPM) to select the best isolate. Mo-blue production was quantified at 865 nm utilizing the extinction coefficient of $16.3 \text{ mM}^{-1} \cdot \text{cm}^{-1}$ to choose the best isolate. Characterization of the molybdenum blue produced was carried out by scanning the absorption spectrum of the blue supernatant from the liquid culture from 400 to 900 nm (UV-spectrophotometer, Shimadzu 1201) with low phosphate media minus bacterium as the baseline correction. Briefly, the culture supernatant was centrifuged at $10,000 \times g$ for 10 minutes at room temperature to remove bacterial aggregates. The bacterium was identified via biochemical and phenotypical methods [23] in accordance to the Bergey's Manual of Determinative Bacteriology [26], and the results plugged into the ABIS online system [27].

Bacterial resting cells preparation

The characterizations of molybdenum reduction including the effects of carbon sources, heavy metals, concentrations of phosphate, molybdate, pH and temperature were carried out utilizing resting cells in a microtiter format as before, but with slight modifications [28]. Briefly, bacterial cells were grown aerobically in several 250 mL shake flasks with shaking at 120 rpm on an

orbital shaker (Yihder, Taiwan) in a volume of 1 L. Incubation was carried out at room temperature. The media utilized was the High Phosphate media (HPM) with the only difference to the LPM was the phosphate concentration set at 100 mM. This was carried out to prevent bacterial aggregations to molybdenum blue, which leads to cellular harvesting complications. Cells were centrifuged at 15,000 x g at 4 °C for 10 minutes. The bacterial pellets were then rinsed with deionized water twice. The pellets were then resuspended in 20 µL of LPM with glucose omitted. Appropriate alterations in the LPM were carried out to meet the needs of modifications in the carbon sources, phosphate, molybdate and pH conditions during the characterization works. About 180 µL of the appropriately modified LPM was sterically transferred into the wells of a sterile microplate. This was followed by the addition of 20 mL of sterile glucose or other carbon sources from a stock solution to the final concentration of 1.0 % (w/v). The total volume was 200 µL. The microplates were then sealed (Corning® microplate), and incubated at room temperature. Readings at 750 nm were periodically taken using a BioRad Microtiter Plate reader (Model No. 680, Richmond, CA). This wavelength is the maximum filter available for the microplate unit [28]. Quantification of the Mo-blue produced was carried out utilizing the extinction coefficient of 11.69 mM⁻¹.cm⁻¹ at 750 nm was utilized to quantify Mo-blue production. The effect of several heavy metals was studied utilizing Atomic Absorption Spectrometry calibration standard solutions from MERCK.

Test of amides and nitriles as sources of electron donor or growth

The capacity of various amides and nitriles to support molybdenum reduction as electron donors was tested using the microplate format above by replacing glucose from the low phosphate medium with nicotinamide, acetamide, iodoacetamide, acrylamide, propionamide, acetamide, acetonitrile, acrylonitrile 2-chloroacetamide, and benzonitrile to the final concentration of 2,000 mg/L [29]. Glucose was the positive control, and was added to the final concentration of 2,000 mg/L. Then 200 µL of the media was added into the microplate wells with 50 µL of resting cells suspension. The microplate was incubated at room temperature for three days and the amount of Mo-blue production was measured at 750 nm as before. The ability of the compounds above to support the growth of this bacterium independent of molybdenum-reduction was tested using the microplate format above using the media below minus molybdate, and replacing glucose with the xenobiotics at the final concentration of 2,000 mg/L in a volume of 50 µL. The ingredients of the growth media (LPM) were as follows: (NH₄)₂·SO₄ (0.3%), NaNO₃ (0.2%), MgSO₄·7H₂O (0.05%), yeast extract (0.01%), NaCl (0.5%) and Na₂HPO₄ (0.705% or 50 mM). Then 200 µL of the media was added into the microplate wells and mixed with 50 µL of resting cells suspension. The media was adjusted to pH 7.0. The increase of bacterial growth was measured at 600 nm after three days of incubation at room temperature.

Mathematical modelling of bacterial growth on amides

Bacterial growth on these xenobiotics was modeled using the modified Gompertz model (Eqn. 1), having three parameters to be solved as this model is frequently used to model microbial growth [16]. where A =bacterial growth at lower asymptote; μ_m = maximum specific bacterial growth rate, λ =lag time, e = exponent (2.718281828) and t = sampling time.

$$y = A \exp \left\{ - \exp \left[\frac{\mu_m e}{A} (\lambda - t) + 1 \right] \right\} \quad (1)$$

RESULTS

Isolation of Mo-reducing bacteria

The ten Mo-reducing bacterial isolates were quantified for their capacity to produce Mo-blue by monitoring production at 865 nm. The best isolate was 6a [Table-1], and was chosen for further studies.

Table: 1. Mo-blue production by bacterial isolates.

Isolate	nmole Mo-blue
1a	0.23
2a	1.87
3a	1.03
4a	0.45
5a	2.19
6a	15.02
7a	3.42
8a	2.13
9a	7.02
10a	3.04

Identification of bacterium

Isolate 6a was a short rod-shaped, motile, Gram-negative bacterium. Identification of the bacterium was carried out by computing the results of cultural, morphological and various biochemical tests [Table-2] into the ABIS online software. Analysis using the software indicated that the bacterial identity giving the highest homology (73%) and accuracy at 91% as *Burkholderia cepacia*. Despite this, molecular identification technique through comparison of the 16srRNA gene is needed to identify this species further. The bacterium is tentatively identified as *Burkholderiasp.* strain Neni-11 in honor of the late Dr. Neni Gusmanizar. The bacterium exhibited optimum pH for reduction of between 6.0 and 6.3, and an optimum temperature ranging from 30 °C to 37°C (Data not shown).

Table: 2. Morphological and biochemical tests of *Burkholderia sp.* strain Neni-11.

Test	Acid production from	
Gram staining	–	:
Motility	+	L-Arabinose +
Growth at 4 °C	–	Citrate +
Growth at 41 °C	+	Fructose +
Growth on MacConkey agar	–	Glucose +
Arginine dihydrolase (ADH)	–	meso-Inositol +
Alkaline phosphatase (PAL)	–	2-Ketogluconate +
H ₂ S production	+	Mannose +
Indole production	+	Mannitol +
Nitrates reduction	–	Sorbitol +
Lecithinase	–	Sucrose +
Lysine decarboxylase (LDC)	+	Trehalose +
Ornithine decarboxylase (ODC)	–	Xylose +
ONPG (beta-galactosidase)	–	Glycogen –
Esculin hydrolysis	+	Methyl-mannoside –
Gelatin hydrolysis	–	D-Melezitose –
Starch hydrolysis	–	Inulin –
Urea hydrolysis	–	Starch –
Oxidase reaction	+	D-Turanose –

Note: + positive result, – negative result

Molybdenum absorbance spectrum

Through the entire progress of molybdate reduction to Mo-blue, scanning of the supernatants of the culture media from 400 to 1000 nm demonstrated that the bacterium showed an exceptional Mo-blue spectrum having a maximum peak at 865 nm and a shoulder at 700 nm. This unique profile was noticed to be conserved through the entire incubation period [Figure- 1].

Effect of electron donor on molybdate reduction

The best electron donor for supporting molybdate reduction was glucose with an optimal concentration at 1% (w/v) (data not shown). This is followed by sorbitol, fructose, 2-ketogluconate, mannose, sucrose, l-arabinose, mannitol, xylose, meso-inositol, trehalose and citrate in descending order [Figure- 2].

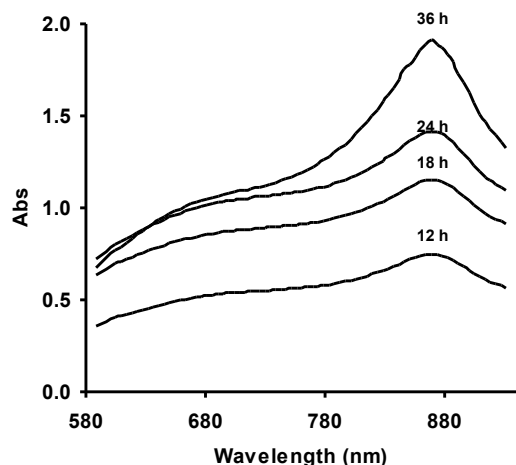


Fig. 1. Scanning absorption spectrum of Mo-blue from *Burkholderiasp.* strain Neni-11 at different time intervals.

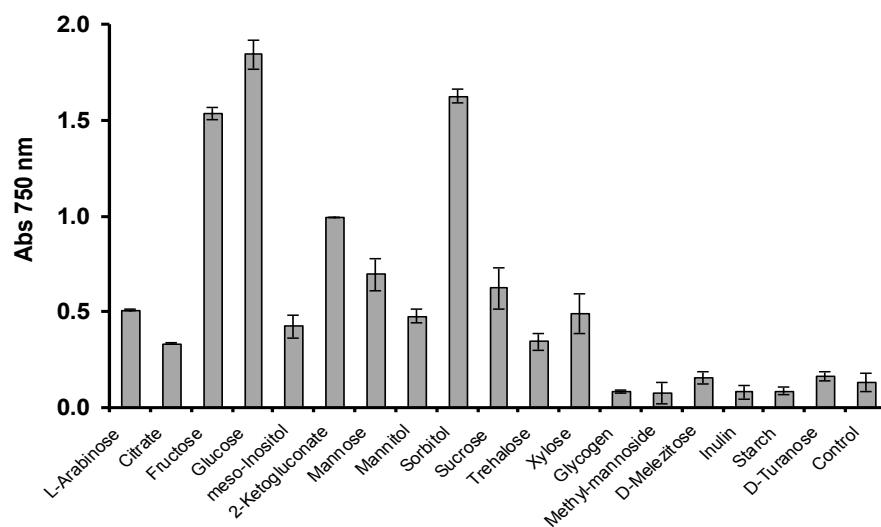


Fig. 2. Mo-blue production utilizing various electron donor sources (1% w/v). The error bars indicate mean \pm standard deviation of three replicates.

Molybdate reduction under various concentrations of phosphate and molybdate

The optimum concentration of phosphate supporting molybdenum reduction occurred between 5.0 and 7.5 mM with higher concentrations were strongly inhibitory to reduction [Figure- 3A]. Maximum amount of Mo-blue produced was seen at concentrations of molybdate at 15 mM, and after an incubation period of 52 hours approximately [Figure- 3B]. A lag period of about 10 hours was observed

Effect of heavy metals

Molybdenum reduction was inhibited by mercury (ii), silver (i) and chromium (vi) at 2 p.p.m. by 91.9, 82.7 and 17.4 %, respectively. The heavy metals arsenic, cadmium, copper and lead did not exhibit inhibition to molybdenum reduction [Figure- 4].

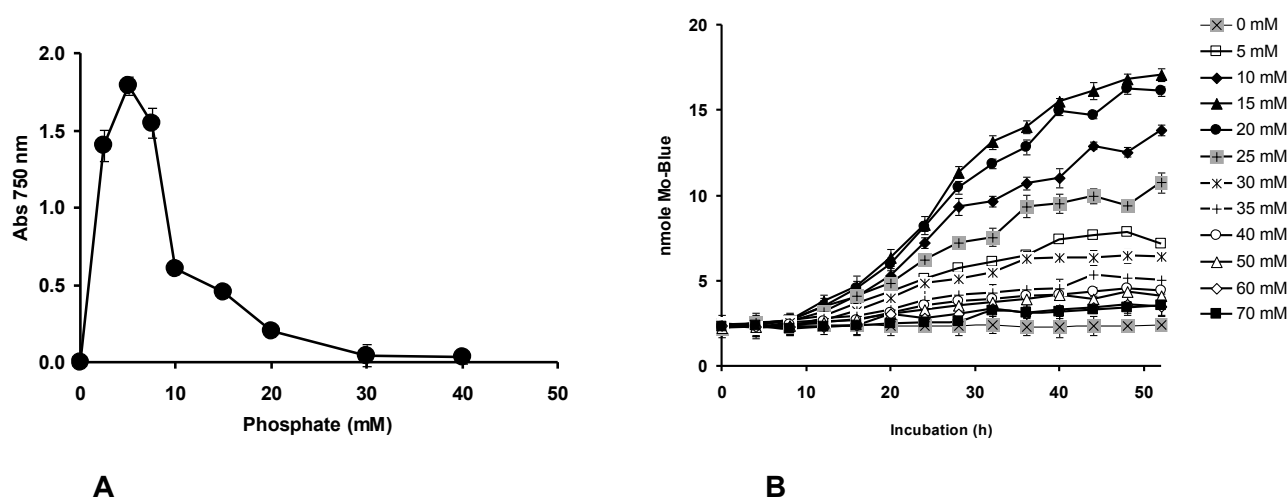


Fig. 3. The effect of phosphate (A) and molybdate (B) concentrations on molybdenum reduction by *Burkholderiasp.* strain Neni-11. The error bars indicate mean \pm standard deviation of three replicates.

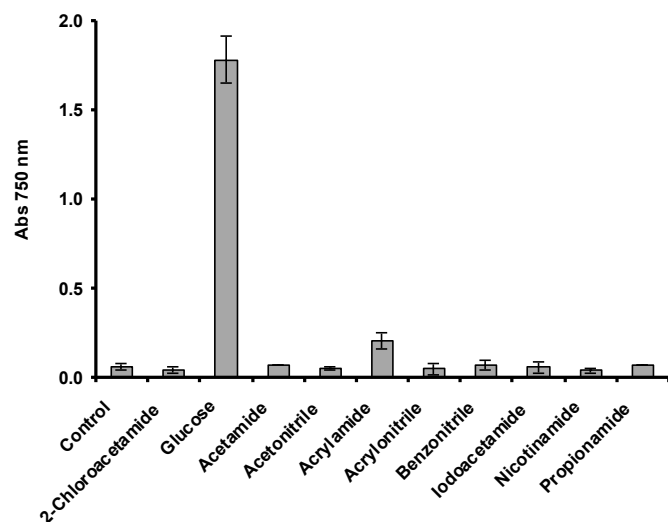


Fig. 4. Mo-blue reduction by xenobiotics at 10 mM in low phosphate media. Glucose was the positive control. The error bars indicate mean \pm standard deviation of three replicates.

Amides and nitriles as electron donors for reduction and growth

The ability of these amides and nitriles to act as electron donor for molybdenum reduction was studied. Only acrylamide was shown to support molybdenum reduction but at a lower efficiency than glucose [Figure-5A]. The amides acrylamide, acetamide and propionamide supported the growth of this bacterium independently of molybdenum reduction [Figure-5B]. The growth of this bacterium on these amides was modelled according to the modified Gompertz model [Figure-6]. The absorbance values at 600 nm were first converted to natural logarithm. The correlation coefficients obtained for the model at 0.99, 0.98 and 0.98 for acrylamide, propionamide and acetamide, respectively, indicated good agreement between predicted and observed values. The growth parameters obtained were maximum specific growth rates of 1.241, 0.971 and 0.85 d⁻¹ for acrylamide, propionamide and acetamide, respectively, while the lag periods of 1.372, 1.562 and 1.639 days were observed for acrylamide, propionamide and acetamide, respectively.

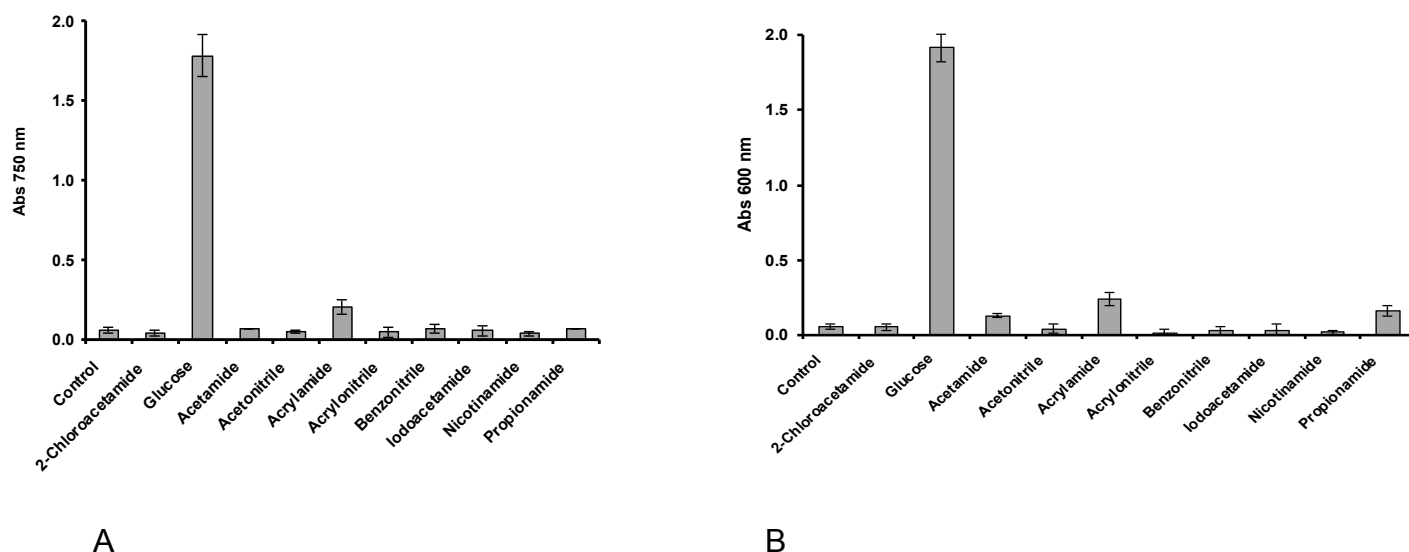


Fig. 5. Mo-blue reduction (A) measured at 750 nm and growth (B) measured at 600 nm by xenobiotics at 10 mM in low phosphate media. Glucose was the positive control. The error bars indicate mean \pm standard deviation of three replicates.

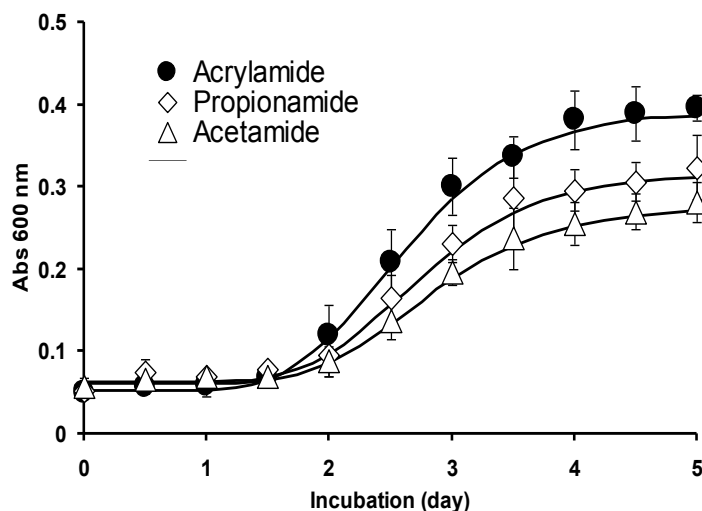


Fig. 6. Growth of *Burkholderiasp.* strain Neni-11 on acrylamide, propionamide and acetamide as modelled using the modified Gompertz model (solid lines). Bacterium was incubated at room temperature in a microtiter plate. The error bars indicate mean \pm standard deviation of three replicates.

DISCUSSION

The phenomenon of molybdenum blue formation from bacterial reduction of molybdenum was first reported in *E. coli* about more than one hundred years ago in 1896 [21]. This is followed in the last century, in 1939 [30]. It was reported again in 1985 after a long absence in *E. coli*K12 [31], and in 1993 in *Enterobacter cloacae* strain 48 [32]. The potential of this phenomenon to be used in the bioremediation of molybdenum is first realized by Ghani et al. [32]. Since then, numerous Mo-reducing bacteria have been isolated [Table-3], including two bacteria that can degrade SDS [23,33] as well as a psychrophilic Mo-reducing bacterium isolated from Antarctica. As the latter is a *Pseudomonas* species, we screened a similar bacterium initially isolated for diesel-degrading capacity to reduce molybdenum to molybdenum blue. This is a second bacterium isolated from Antarctica showing molybdenum-

reducing property. The microtiter plate format utilizing resting cells allows a high throughput characterization format [23,28,34]. The utilization of resting cells or whole cells was first initiated in the bacterium *Enterobacter cloacae* strain 48 [32]. Several bacterial characterizations work such as in selenate [35], chromate [36] and vanadate [37] reductions also utilize resting cells. Furthermore, biodegradation of xenobiotics for example SDS [38,39] and diesel [40] also takes advantage of resting cells. The use of resting cells bypasses the initial stage of the growth process that is normally affected by toxic xenobiotics.

In the past, Mo-blue production by Mo-reducing bacteria has been hypothesized to commence initially by an enzymatic reduction from the Mo^{6+} to the Mo^{5+} oxidation state. This is eventually accompanied by the add-on of phosphate ions from the surroundings producing Mo-blue [32]. However, this mechanism has some issues. In reality, Mo^{6+} ion does not exist in liquid solution. At neutral pH, molybdate appears as $[\text{MoO}_4]^{2-}$ or molybdate anions with its protonated form, either HMoO_4^- or H_2MoO_4 . Molybdate concentrations of above 1 mM and at acidic pHs, molybdate ions instantly formed polyions among others $\text{H}_2\text{Mo}_7\text{O}_{24}^{4-}$, $\text{HMo}_7\text{O}_{24}^{5-}$, $\text{Mo}_7\text{O}_{24}^{6-}$, and $\text{Mo}_{12}\text{O}_{37}^{2-}$. At very acidic pHs (<2.0), species such as $\text{Mo}_8\text{O}_{26}^{4-}$ and $\text{Mo}_{36}\text{O}_{112}(\text{H}_2\text{O})_{16}^{8-}$ started to form with even complex species forming with further acidification. These forms of molybdenum are called polyoxomolybdates. The structure can incorporate heteroatoms such as silicate or phosphate, in the latter forming heteropolyoxomolybdates [51]. Enzymes for examples aldehyde oxidase and xantine oxidase can reduce these compounds into Mo-blue, which is an intense colloidal product with fractional oxidation state [52]. Nearly all bacterially produced Mo-blue show spectra with close similarity to the phosphate determination method [23,53], the latter is a reduced phosphomolybdate having a characteristics shoulder of from 700 to 720 nm, and a peak maximum from 870 nm to 890 nm [52,54]. We put forward a new hypothesis on Mo-blue production in bacteria based on molybdenum chemistry and Mo-blue spectral analysis that a phosphomolybdate intermediate is formed during the reduction of sodium molybdate to Mo-blue in bacteria [53]. The presence of an intermediate species during heavy metal reduction has been reported in chromate reduction ($6+$ to $3+$) at least in the bacteria *Pseudomonas ambigua* [55] and *Shewanella putrefaciens* (now known as *S. oneidensis*) [56], where spectroscopic and paramagnetic resonance works have confirmed the presence of the intermediate species Cr^{5+} . Spectroscopic analysis employed in this work is regarded as a simple method for distinguishing between the existing heteropolyoxomolybdates, which include silicomolybdate, phosphomolybdate, and sulfomolybdate. On the other hand, additional investigations making use of nuclear magnetic resonance and electron spin resonance are essential for in depth identification of the precise lacunary species of phosphomolybdate associated with bacterial reduction of molybdenum [52, 57].

The majority of the molybdenum reducers prefer either glucose or sucrose as the best carbon source **Table- 3**. One of the reasons is the easily assimilable characteristics of these carbohydrates. With generic metabolic pathways, the reducing equivalents NADH and NADPH can be generated easily using these carbon sources. Both of these compounds are electron-donating substrates for the molybdenum reducing-enzyme [58,59]. Despite sucrose and glucose being excellent electron donor, a cheaper carbon source for example molasses can be utilized especially in actual bioremediation, since molasses can be obtained economically and in large quantity from the sugar cane industry in Malaysia [60]. Molasses has been utilized as electron donor in the reduction of hexavalent chromate by the bacterium *Flexivirga alba* [61] and selenate reduction by five bacterial isolates [62]. The possible utilization of molasses as a carbon source is currently being evaluated.

The presence of this lag period is probably because the conversion of molybdate to the intermediate phosphomolybdate needs to reach a critical value before reduction can take place as discussed previously [19]. It has been reported that bacterial molybdenum reduction is inhibited by phosphate at concentrations higher than 2.9 mM [32]. In general, concentrations higher than 5 mM are inhibitory to many Mo-reducing bacteria [Table-3]. Phosphomolybdate is rapidly oxidized at neutral pHs, and its stability requires acidic pH [63]. At concentrations of 20 mM and higher, phosphate maintains the environment at neutrality. This rapidly destabilizes phosphomolybdate. Phosphate itself can destabilize the phosphomolybdate complex as a study has demonstrated that an acidified phosphate solution destabilizes an ascorbate-reduced phosphomolybdate [64].

The concentrations of molybdate supporting optimal Mo-blue production in bacteria range between 5 and 80 mM [Table-3]. In contrast to cationic heavy metals, bacteria can tolerate and reduce high concentrations of anionic heavy metals. For instance, the most tolerant microorganism can tolerate and reduce arsenate at 30 mM in *Desulfomicrobium strain Ben-RB* [65], chromate at 30 mM in *Pseudomonas putida* [66], selenate at 20 mM in *Bacillus sp.* [67], and vanadate at 50 mM in *Pseudomonas isachenkovii* [68]. These bacteria can be employed to cleanup molybdenum-polluted areas with high concentrations of molybdenum. A number of areas are stated to be polluted with high concentrations of molybdenum. In Colorado, contaminated sites from a discontinued uranium mine show molybdenum concentration as much as 6,500 mg/Kg in soils and 900 mg/L in water [69]. For efficient

reduction to take place, the phosphate concentrations should not exceed 20 mM. It is fortunate that most sites do not contain phosphate at concentrations exceeding this value [70].

Table: 3. Characterization of Mo-reducing bacteria isolated to date.

Bacteria	Optimal C source	Optimal Molybdate (mM)	Optimal Phosphate (mM)	Heavy metals inhibition	Author
<i>Klebsiella oxytoca</i> strain Aft-7	glucose	5-20	5-7.5	Cu ²⁺ , Ag ⁺ , Hg ²⁺	[23]
<i>Bacillus pumilus</i> strain lbna	glucose	40	2.5-5	As ³⁺ , Pb ²⁺ , Zn ²⁺ , Cd ²⁺ , Cr ⁶⁺ , Hg ²⁺ , Cu ²⁺	[41]
<i>Bacillus</i> sp. strain A.rzi	glucose	50	4	Cd ²⁺ , Cr ⁶⁺ , Cu ²⁺ , Ag ⁺ , Pb ²⁺ , Hg ²⁺ , Co ²⁺ , Zn ²⁺	[42]
<i>Serratia</i> sp. strain Dr.Y8	sucrose	50	5	Cr, Cu, Ag, Hg	[43]
<i>S. marcescens</i> strain Dr.Y9	sucrose	20	5	Cr ⁶⁺ , Cu ²⁺ , Ag ⁺ , Hg ²⁺	[44]
<i>Serratia</i> sp. strain Dr.Y5	glucose	30	5	n.a.	[45]
<i>Pseudomonas</i> sp. strain DRY2	glucose	15-20	5	Cr ⁶⁺ , Cu ²⁺ , Pb ²⁺ , Hg ²⁺	[46]
<i>Pseudomonas</i> sp. strain DRY1	glucose	30-50	5	Cd ²⁺ , Cr ⁶⁺ , Cu ²⁺ , Ag ⁺ , Pb ²⁺ , Hg ²⁺	[22]
<i>Enterobacter</i> sp. strain Dr.Y13	glucose	25-50	5	Cr ⁶⁺ , Cd ²⁺ , Cu ²⁺ , Ag ⁺ , Hg ²⁺	[47]
<i>Acinetobacter calcoaceticus</i> strain Dr.Y12	glucose	20	5	Cd ²⁺ , Cr ⁶⁺ , Cu ²⁺ , Pb ²⁺ , Hg ²⁺	[48]
<i>Serratia marcescens</i> strain DRY6	sucrose	15-25	5	Cr ⁶⁺ , Cu ²⁺ , Hg ²⁺	[49]
<i>Enterobacter cloacae</i> strain 48	sucrose	20	2.9	Cr ⁶⁺ , Cu ²⁺	[32]
<i>Escherichia coli</i> K12	glucose	80	5	Cr ⁶⁺	[31]
<i>Klebsiella oxytoca</i> strain hkeem	fructose	80	4.5	Cu ²⁺ , Ag ⁺ , Hg ²⁺	[50]

Two of the heavy metals tested that exhibit strong inhibitory response to molybdenum reduction, mercury and chromium, inhibit many of the Mo-reducing bacteria isolate to date [Table- 3]. Mercury is a strong inhibitor to bacterial chromate reduction from Cr⁶⁺ to Cr³⁺ in *Bacillus* sp. with the target site of inhibition is proposed as the sulfhydryl group [71]. Chromate inhibits the enzyme glucose oxidase [72] and nitrogen metabolism enzymes [73]. The addition of certain metal-sequestering or chelating substances such as calcium carbonate, manganese oxide, phosphate, and magnesium hydroxide to bioremediation sites may overcome the problem of mercury inhibition [74], and allowing molybdenum remediation to proceed. Another alternative to reduce the toxicity of mercury and copper is to immobilize the molybdenum-reducing bacterium in membrane or dialysis tubing [20].

The growth rate obtained indicates that growth on acrylamide was faster than either acetamide or propionamide, while the lag period observed also indicates that the bacteria could grow on acrylamide faster with a lower lag period than acetamide and propionamide. The presence of lag periods indicates that the bacterial cells spend energy to tolerate and activate metabolic pathways needed for amide assimilation. The ability of acrylamide to support Mo-reduction is novel. In the reduction of chromate, the xenobiotic phenol could be used as electron donor [75]. However, these two phenomena are very rare as most of the time simple carbohydrates such as lactate, sucrose or glucose are preferred donors [19]. The amides acrylamide, acetamide and propionamide are manufactured in the millions of tons annually. As the pollution of these amides is increasingly being reported, ways to remediate them are being sought. To date, several microorganisms have been isolated that can use these amides as carbon or nitrogen sources for growth. These microorganisms are potential bioremediation candidates [15,16,24,76–84]. Nonetheless, hardly any bacteria have been mentioned capable of degrading amide and detoxify heavy metals. Thus, the potential of this bacterium to accomplish the two functions shows that this bacterium can be beneficial as a bioremediation agent in contaminated sites co-contaminated with amides and heavy metals.

CONCLUSION

A molybdenum-reducing bacterium showing the novel ability to use acrylamide as a source of electron donor for reduction is reported. In addition, the amides acrylamide, propionamide, and acetamide can be utilized as the growth of this bacterium. Characterization of molybdenum reduction including screening of potential xenobiotics acting as electron donor or carbon sources for growth was carried out utilizing resting cells in a microplate format allowing a potentially high throughput process. Glucose was the best electron donor for supporting reduction, while a critical phosphate concentration of 5.0 mM was optimal. Higher concentrations of phosphate were strongly inhibitory. The identity of the molybdenum blue produced indicated that it is a reduced phosphomolybdate based on scanning absorption spectrum. A modified Gompertz model was successfully used in modelling the growth of this bacterium on these amides. Nonetheless, hardly any bacteria have been mentioned capable of degrading amide and detoxify heavy metals. Thus, the potential of this bacterium to accomplish the two functions shows that this bacterium can be beneficial as a bioremediation agent in contaminated sites co-contaminated with amides and heavy metals.

CONFLICT OF INTEREST

The author declares having no competing interests.

ACKNOWLEDGEMENT

A portion of this project was supported by funds from Snoc International Sdn Bhd.

FINANCIAL DISCLOSURE

Institutional Support was received.

REFERENCES

- [1] Apte SC, Kwong YT. [2003] Deep sea tailings placement: critical review of environmental issues. CSIRO Australia and CANMET Canada
- [2] Angel BM, Simpson SL, Jarolimek CV, Jung R, Waworuntu J, Batterham G. [2013] Trace metals associated with deep-sea tailings placement at the Batu Hijau copper-gold mine, Sumbawa, Indonesia. *Mar Pollut Bull* 73:306–313.
- [3] Yu C, Xu S, Gang M, Chen G, Zhou L. [2011] Molybdenum pollution and speciation in Nver river sediments impacted with Mo mining activities in Western Liaoning, northeast China. *Int J Environ Res* 5:205–212.
- [4] Simeonov LI, Kochubovski MV, Simeonova BG. [2011] Environmental heavy metal pollution and effects on child mental development. Springer Netherlands, Dordrecht
- [5] Kargar M, Khorasani N, Karami M, Rafiee G-R, Naseh R. [2011] Study of aluminum, copper and molybdenum pollution in groundwater sources surrounding (Miduk) Shahr-e- Babak copper complex tailings dam. *World Acad Sci Eng Technol* 76:412–416.
- [6] Ali MF, Lee YH, Ratnam W, Nais J, Ripin R. [2006] The content and accumulation of arsenic and heavy metals in medicinal plants near Mamut River contaminated by copper-mining in Sabah, Malaysia. *Fresenius Environ Bull* 15:1316–1321.
- [7] Mohammad Ali BN, Lin CY, Cleophas F, Abdullah MH, Musta B. [2015] Assessment of heavy metals contamination in Mamut river sediments using sediment quality guidelines and geochemical indices. *Environ Monit Assess*. doi: 10.1007/s10661-014-4190-y
- [8] Kessler KL, Olson KC, Wright CL, Austin KJ, Johnson PS, Cammack KM. [2012] Effects of supplemental molybdenum on animal performance, liver copper concentrations, ruminal hydrogen sulfide concentrations, and the appearance of sulfur and molybdenum toxicity in steers receiving fiber-based diets. *J Anim Sci* 90:5005–5012.
- [9] Chopikashvili LV, Bobyleva LA, Zolotareva GN. [1991] Genotoxic effects of molybdenum and its derivatives in an experiment on *Drosophila* and mammals. *Tsitol Genet* 25:45–49.
- [10] Pandey G, Jain GC. [2015] Molybdenum induced histopathological and histomorphometric alterations in testis of male Wistar rats. *Int J Curr Microbiol Appl Sci* 4:150–161.
- [11] Yamaguchi S, Miura C, Ito A, Agusa T, Iwata H, Tanabe S, Tuyen BC, Miura T. [2007] Effects of lead, molybdenum, rubidium, arsenic and organochlorines on spermatogenesis in fish: Monitoring at Mekong Delta area and in vitro experiment. *Aquat Toxicol* 83:43–51.
- [12] Narra MR, Begum G, Rajender K, Venkateswara Rao J. [2012] Toxic impact of two organophosphate insecticides on biochemical parameters of a food fish and assessment of recovery response. *Toxicol Ind Health* 28:343–352.
- [13] Ahmad WA, Wan Ahmad WH, Karim NA, Santhana Raj AS, Zakaria ZA [2013] Cr(VI) reduction in naturally rich growth medium and sugarcane bagasse by *Acinetobacter haemolyticus*. *Int Biodeterior Biodegrad* 85:571–576.
- [14] Sing NN, Zulkharnain A, Roslan HA, Assim Z, Husaini A. [2014] Bioremediation of PCP by *Trichoderma* and *Cunninghamella* strains isolated from sawdust. *Braz Arch Biol Technol* 57:811–820.
- [15] Rahim MBH, Syed MA, Shukor MY. [2012] Isolation and characterization of an acrylamide-degrading yeast *Rhodotorula* sp. strain MBH23 KCTC 11960BP. *J Basic Microbiol* 52:573–581.
- [16] Shukor MY, Gusmanizar N, Ramli J, Shamaan NA, MacCormack WP, Syed MA. [2009] Isolation and

- characterization of an acrylamide-degrading Antarctic bacterium. *J Environ Biol* 30:107–112.
- [17] Rogacheva SM, Ignatov OV. [2001] The respiratory activity of *Rhodococcus rhodochromis* M8 cells producing nitrile-hydrolyzing enzymes. *Appl Biochem Microbiol* 37:282–286.
- [18] Smith EA, Prues SL, Oehme FW. [1996] Environmental degradation of polyacrylamides. 1. Effects of artificial environmental conditions: Temperature, light, and pH. *Ecotoxicol Environ Saf* 35:121–135.
- [19] Shukor MY, Syed MA. [2010] Microbiological reduction of hexavalent molybdenum to molybdenum blue. *Curr. Res. Technol. Educ Top Appl Microbiol Microbiotechnol* 2:
- [20] Halmi MIE, Wasoh H, Sukor S, Ahmad SA, Yusof MT, Shukor MY. [2014] Bioremoval of molybdenum from aqueous solution. *Int J Agric Biol* 16:848–850.
- [21] Capaldi A, Proskauer B. [1896] Beiträge zur Kenntniss der Säurebildung bei *Typhus-bacillen* und *Bacterium coli* - Eine differential-diagnostische Studie. *Z Für Hyg Infect* 23:452–474.
- [22] Ahmad SA, Shukor MY, Shamaan NA, Mac Cormack WP, Syed MA. [2013] Molybdate reduction to molybdenum blue by an Antarctic bacterium. *BioMed Res Int*. doi: 10.1155/2013/871941
- [23] Masdor N, Abd Shukor MS, Khan A, Bin Halmi MIE, Abdullah SRS, Shamaan NA, Shukor MY. [2015] Isolation and characterization of a molybdenum-reducing and SDS-degrading *Klebsiella oxytoca* strain Aft-7 and its bioremediation application in the environment. *Biodiversitas* 16:238–246.
- [24] Buranasilp K, Charoenpanich J. [2011] Biodegradation of acrylamide by *Enterobacter aerogenes* isolated from wastewater in Thailand. *J Environ Sci* 23:396–403.
- [25] Bhattacharya A, Gupta A, Kaur A, Malik D. [2014] Efficacy of *Acinetobacter* sp. B9 for simultaneous removal of phenol and hexavalent chromium from co-contaminated system. *Appl Microbiol Biotechnol* 98:9829–9841.
- [26] Holt JG, Krieg NR, Sneath PHA, Staley JT, Williams ST. [1994] *Bergey's Manual of Determinative Bacteriology*, 9th ed. Lippincott Williams & Wilkins
- [27] Costin S, Ionut S. [2015] ABIS online - bacterial identification software, http://www.tgw1916.net/bacteria_logare.html, database version: *Bacillus* 022012-2.10, accessed on Mar 2015.
- [28] Shukor MS, Shukor MY. [2014] A microplate format for characterizing the growth of molybdenum-reducing bacteria. *J Environ Microbiol Toxicol* 2:42–44.
- [29] Arif NM, Ahmad SA, Syed MA, Shukor MY. [2013] Isolation and characterization of a phenol-degrading *Rhodococcus* sp. strain AQ5NOL 2 KCTC 11961BP. *J Basic Microbiol* 53:9–19.
- [30] Jan A [1939] La reduction biologique du molybdate d'ammonium par les bactéries du genre *Serratia* (The biological reduction of ammonium molybdate by the bacteria of the *Serratia* kind). *Bull Sci Pharmacol* 46:336–339.
- [31] Campbell AM, Del Campillo-Campbell A, Villaret DB. [1985] Molybdate reduction by *Escherichia coli* K-12 and its chl mutants. *Proc Natl Acad Sci U S A* 82:227–231.
- [32] Ghani B, Takai M, Hisham NZ, Kishimoto N, Ismail AKM, Tano T, Sugio T. [1993] Isolation and characterization of a Mo⁶⁺-reducing bacterium. *Appl Environ Microbiol* 59:1176–1180.
- [33] Halmi MIE, Zuhainis SW, Yusof MT, Shaharuddin NA, Helmi W, Shukor Y, Syed MA, Ahmad SA. [2013] Hexavalent molybdenum reduction to Mo-blue by a sodium-dodecyl-sulfate- degrading *Klebsiella oxytoca* strain dry14. *BioMed Res Int* 2013:8 pages.
- [34] Iyamu EW, Asakura T, Woods GM. [2008] A colorimetric microplate assay method for high-throughput analysis of arginase activity in vitro. *Anal Biochem* 383:332–334.
- [35] Losi ME, Jr WTF. [1997] Reduction of selenium oxyanions by *Enterobacter cloacae* strain SLD1a-1: Reduction of selenate to selenite. *Environ Toxicol Chem* 16:1851–1858.
- [36] Llovera S, Bonet R, Simon-Pujol MD, Congregado F. [1993] Chromate reduction by resting cells of *Agrobacterium radiobacter* EPS-916. *Appl Environ Microbiol* 59:3516–3518.
- [37] Carpentier W, Smet LD, Beeumen JV, Brigé A. [2005] Respiration and growth of *Shewanella oneidensis* MR-1 using vanadate as the sole electron acceptor. *J Bacteriol* 187:3293–3301.
- [38] Chaturvedi V, Kumar A. [2011] Diversity of culturable sodium dodecyl sulfate (SDS) degrading bacteria isolated from detergent contaminated ponds situated in Varanasi city, India. *Int Biodeterior Biodegrad* 65:961–971.
- [39] Venkatesh C. [2013] A plate assay method for isolation of bacteria having potent Sodium Doecyl Sulfate (SDS) degrading ability. *Res J Biotechnol* 8:27–31.
- [40] Auffret MD, Yergeau E, Labbé D, Fayolle-Guichard F, Greer CW. [2015] Importance of *Rhodococcus* strains in a bacterial consortium degrading a mixture of hydrocarbons, gasoline, and diesel oil additives revealed by metatranscriptomic analysis. *Appl Microbiol Biotechnol* 99:2419–2430.
- [41] Abo-Shakeer LKA, Ahmad SA, Shukor MY, Shamaan NA, Syed MA. [2013] Isolation and characterization of a molybdenum-reducing *Bacillus pumilus* strain lbna. *J Environ Microbiol Toxicol* 1:9–14.
- [42] Othman AR, Bakar NA, Halmi MIE, Johari WLW, Ahmad SA, Jirangon H, Syed MA, Shukor MY. [2013] Kinetics of molybdenum reduction to molybdenum blue by *Bacillus* sp. strain A.rzi. *BioMed Res Int*. doi: 10.1155/2013/371058
- [43] Shukor MY, Rahman MF, Suhaili Z, Shamaan NA, Syed MA. [2009] Bacterial reduction of hexavalent molybdenum to molybdenum blue. *World J Microbiol Biotechnol* 25:1225–1234.
- [44] Yunus SM, Hamim HM, Anas OM, Aripin SN, Arif SM. [2009] Mo (VI) reduction to molybdenum blue by *Serratia marcescens* strain Dr. Y9. *Pol J Microbiol* 58:141–147.
- [45] Rahman MFA, Shukor MY, Suhaili Z, Mustafa S, Shamaan NA, Syed MA. [2009] Reduction of Mo(VI) by the bacterium *Serratia* sp. strain DRY5. *J Environ Biol* 30:65–72.
- [46] Shukor MY, Ahmad SA, Nadzir MMM, Abdullah MP, Shamaan NA, Syed MA. [2010] Molybdate reduction by *Pseudomonas* sp. strain DRY2. *J Appl Microbiol* 108:2050–2058.
- [47] Shukor MY, Rahman MF, Shamaan NA, Syed MS. [2009] Reduction of molybdate to molybdenum blue by *Enterobacter* sp. strain Dr.Y13. *J Basic Microbiol* 49:S43–S54.
- [48] Shukor MY, Rahman MF, Suhaili Z, Shamaan NA, Syed MA. [2010] Hexavalent molybdenum reduction to Mo-blue by *Acinetobacter calcoaceticus*. *Folia Microbiol (Praha)* 55:137–143.
- [49] Shukor MY, Habib SHM, Rahman MFA, Jirangon H, Abdullah MPA, Shamaan NA, Syed MA. [2008] Hexavalent molybdenum reduction to molybdenum blue by *S. marcescens* strain Dr. Y6. *Appl Biochem Biotechnol* 149:33–43.
- [50] Lim HK, Syed MA, Shukor MY. [2012] Reduction of molybdate to molybdenum blue by *Klebsiella* sp. strain hkeem. *J Basic Microbiol* 52:296–305.
- [51] Krishnan CV, Garnett M, Chu B. [2008] Influence of pH and acetate on the self-assembly process of

- (NH₄)₄₂.Mo^{VI}₇₂Mo^V₆₀O₃₇₂(CH₃COO)₃₀(H₂O)₇₂.ca.300H₂O. *Int J Electrochem Sci* 3:1299–1315.
- [52] Kazansky LP, Fedotov MA. [1980] Phosphorus-³¹ and oxygen-¹⁷ N.M.R. evidence of trapped electrons in reduced 18-molybdodiphosphate(V), P₂Mo₁₈O₆₂⁸⁻. *J Chem Soc Chem Commun* 14:644–646.
- [53] Shukor Y, Adam H, Ithnin K, Yunus I, Shamaan NA, Syed A. [2007] Molybdate reduction to molybdenum blue in microbe proceeds via a phosphomolybdate intermediate. *J Biol Sci* 7:1448–1452.
- [54] Clesceri LS, Greenberg AE, Trussell RR. [1989] Standard methods for the examination of water and wastewater. Port City Press, Baltimore
- [55] Suzuki T, Miyata N, Horitsu H, Kawai K, Takamizawa K, Tai Y, Okazaki M. [1992] NAD(P)H-dependent chromium(VI) reductase of *Pseudomonas ambigua* G-1: A Cr(V) intermediate is formed during the reduction of Cr(VI) to Cr(III). . 174:5340–5345.
- [56] Myers CR, Carstens BP, Antholine WE, Myers JM. [2000] Chromium(VI) reductase activity is associated with the cytoplasmic membrane of anaerobically grown *Shewanella putrefaciens* MR-1. *J Appl Microbiol* 88:98–106.
- [57] Sims RPA [1961] Formation of heteropoly blue by some reduction procedures used in the micro-determination of phosphorus. *The Analyst* 86:584–590.
- [58] Shukor MY, Rahman MFA, Shamaan NA, Lee CH, Karim MIA, Syed MA. [2008] An improved enzyme assay for molybdenum-reducing activity in bacteria. *Appl Biochem Biotechnol* 144:293–300.
- [59] Shukor MY, Halmi MIE, Rahman MFA, Shamaan NA, Syed MA. [2014] Molybdenum reduction to molybdenum blue in *Serratia* sp. strain DRY5 is catalyzed by a novel molybdenum-reducing enzyme. *BioMed Res Int*. doi: 10.1155/2014/853084
- [60] El-Gendy NS, Madian HR, Amr SSA. [2013] Design and optimization of a process for sugarcane molasses fermentation by *Saccharomyces cerevisiae* using response surface methodology. *Int J Microbiol* 2013:9.
- [61] Sugiyama T, Sugito H, Mamiya K, Suzuki Y, Ando K, Ohnuki T. [2012] Hexavalent chromium reduction by an actinobacterium *Flexivirga alba* ST13T in the family Dermacoccaceae. *J Biosci Bioeng* 113:367–371.
- [62] Zhang Y, Okeke BC, Jr WTF. [2008] Bacterial reduction of selenate to elemental selenium utilizing molasses as a carbon source. *Bioresour Technol* 99:1267–1273.
- [63] Glenn JL, Crane FL. [1956] Studies on metalloflavoproteins. V. The action of silicomolybdate in the reduction of cytochrome c by aldehyde oxidase. *Biochim Biophys Acta* 22:111–115.
- [64] Shukor MY, Syed MA, Lee CH, Karim MIA, Shamaan NA. [2002] A method to distinguish between chemical and enzymatic reduction of molybdenum in *Enterobacter cloacae* strain 48. *Malays J Biochem* 7:71–72.
- [65] Macy JM, Santini JM, Pauling BV, O'Neill AH, Sly LI. [2000] Two new arsenate/sulfate-reducing bacteria: Mechanisms of arsenate reduction. 173:49–57.
- [66] Keyhan M, Ackerley DF, Matin A. [2003] Targets of improvement in bacterial chromate bioremediation. *Remediat. Contam. Sediments*
- [67] Fujita M, Ike M, Nishimoto S, Takahashi K, Kashiwa M. [1997] Isolation and characterization of a novel selenate-reducing bacterium, *Bacillus* sp. SF-1. *J Ferment Bioeng* 83:517–522.
- [68] Antipov AN, Lyalikova NN, Khijniak TV, L'vov NP. [2000] Vanadate reduction by molybdenum-free dissimilatory nitrate reductases from vanadate-reducing bacteria. *IUBMB Life* 50:39–42.
- [69] Stone J, Stetler L. [2008] Environmental Impacts from the North Cave Hills Abandoned Uranium Mines, South Dakota. In: Merkel B, Hasche-Berger A (eds) Uranium Min. Hydrogeol. Springer Berlin Heidelberg, pp 371–380
- [70] Jenkins SH. [1973] Phosphorus in fresh water and the marine environment. *Biol Conserv* 5:95.
- [71] Elangovan R, Abhipsa S, Rohit B, Ligy P, Chandraraj K. [2006] Reduction of Cr(VI) by a *Bacillus* sp. *Biotechnol Lett* 28:247–252.
- [72] Zeng G-M, Tang L, Shen G-L, Huang G-H, Niu C-G. [2004] Determination of trace chromium (VI) by an inhibition-based enzyme biosensor incorporating an electropolymerized aniline membrane and ferrocene as electron transfer mediator. *Int J Environ Anal Chem* 84:761–774.
- [73] Sangwan P, Kumar V, Joshi UN. [2014] Effect of chromium(VI) toxicity on enzymes of nitrogen metabolism in clusterbean (*Cyamopsis tetragonoloba* L.). *Enzyme Res* 2014:784036.
- [74] Hettiarachchi GM, Pierzynski GM, Ransom MD. [2000] In situ stabilization of soil lead using phosphorus and manganese oxide. *Environ Sci Technol* 34:4614–4619.
- [75] Anu M, Salom Gnana TV, Reshma JK. [2010] Simultaneous phenol degradation and chromium (VI) reduction by bacterial isolates. *Res J Biotechnol* 5:46–49.
- [76] Nawaz MS, Billedeau SM, Cerniglia CE. [1998] Influence of selected physical parameters on the biodegradation of acrylamide by immobilized cells of *Rhodococcus* sp. *Biodegradation* 9:381–387.
- [77] Shukor MY, Gusmanizar N, Azmi NA, Hamid M, Ramli J, Shamaan NA, Syed MA. [2009] Isolation and characterization of an acrylamide-degrading *Bacillus cereus*. *J Environ Biol* 30:57–64.
- [78] Cha M, Chambliss GH [2011] Characterization of acrylamidase isolated from a newly isolated acrylamide-utilizing bacterium, *Ralstonia eutropha* AUM-01. *Curr Microbiol* 62:671–678.
- [79] Syed MA, Ahmad SA, Kusnin N, Shukor MYA. [2012] Purification and characterization of amidase from acrylamide-degrading bacterium *Burkholderia* sp. strain DR.Y27. *Afr J Biotechnol* 11:329–336.
- [80] Thanyacharoen U, Tani A, Charoenpanich J. [2012] Isolation and characterization of *Kluyvera georgiana* strain with the potential for acrylamide biodegradation. *J Environ Sci Health - Part Toxic-Hazard Subst Environ Eng* 47:1491–1499.
- [81] Jebasingh SEJ, Lakshmikandan M, Rajesh RP, Raja . [2013] Biodegradation of acrylamide and purification of acrylamidase from newly isolated bacterium *Moraxella osloensis* MSU11. *Int Biodeterior Biodegrad* 85:120–125.
- [82] Liu Z-H, Cao Y-M, Zhou Q-W, Guo K, Ge F, Hou J-Y, Hu S-Y, Yuan S, Dai Y-J. [2013] Acrylamide biodegradation ability and plant growth-promoting properties of *Variovorax boronicumulans* CGMCC 4969. *Biodegradation* 24:855–864.
- [83] Chandrashekar V, Chandrashekar C, Shivakumar R, Bhattacharya S, Das A, Gouda B, Rajan SS. [2014] Assessment of acrylamide degradation potential of *Pseudomonas aeruginosa* BAC-6 isolated from industrial effluent. *Appl Biochem Biotechnol* 173:1135–1144.
- [84] Lakshmikandan M, Sivaraman K, Raja SE, Vasanthakumar P, Rajesh RP, Sowparthani K, Jebasingh SEJ. [2014] Biodegradation of acrylamide by acrylamidase from *Stenotrophomonas acidaminiphila* MSU12 and analysis of

degradation products by MALDI-TOF and HPLC. *Int Biodeterior Biodegrad* 94:214–221.

ABOUT AUTHORS



Ir. Dr. Rusnam Mansur received his PhD from Universiti Putra Malaysia in 2007, and is currently a senior lecturer in the Department of Agricultural Technology, Faculty of Agriculture, Padang, 25163, Indonesia. His main interests are agricultural technology and biotechnology



The late Dr. Neni Gusmanizar earned her doctorate in 2007 from Universiti Putra Malaysia. Then she worked as an academician in the Department of Animal Nutrition, Faculty of Animal Science, Andalas University, Padang, Indonesia, specializing in animal microbiology and biotechnology before passing away in 2011. Her loss is greatly missed.



Mr. Mohd. Shukri Abd. Shukor earned his Bachelor of Engineering from the University of Manchester Institute of Science and Technology (UMIST), now University of Manchester. He is currently the CEO at Snoc International Sdn. Bhd, a company involving in trading and research in the field of agriculture and biotechnology.



Muhamad Akhmal Hakim Bin Roslan earned a Bachelor of Sciences Degree in Biochemistry in 2012. He is currently pursuing his PhD in Animal Production with a focus on sustainable animal feed at Institute of Tropical Agriculture, UPM. Akhmal Hakim is the CEO at Halways Sdn Bhd, a start-up under UPM Innohub Programme for technology commercialization.



Assoc. Prof. Mohd. Yunus Abd. Shukor (Orcid ID <http://orcid.org/0000-0002-6150-2114>) is a researcher from Universiti Putra Malaysia. His areas of interest are biochemistry and biotechnology specializing in environmental biotechnology



Mrs. Noor Azlina Masdor earned her BSc and MSc from Universiti Putra Malaysia. She is currently a senior researcher in the Malaysian Agricultural Research and Development Institute (MARDI). Her fields are biodiagnostics and biotechnology.



Siti Aqlima Ahmad is a senior lecturer and course coordinator in the field of biochemistry and environmental toxicology at the Faculty of Biotechnology and Biomolecular Sciences, Universiti Putra Malaysia. She received her Bac. Sci. (Hons), Master and PhD in biochemistry from Universiti Putra Malaysia. Currently, she teaches the subjects environmental biochemistry, enzymology and industrial biochemistry at Universiti Putra Malaysia. Siti Aqlima has 10 years' experience in researching the subjects of environmental toxicology and has produced more than 30 journals in scopus and ISI-cited journals. Her main research interest is the bioremediation of heavy metals and xenobiotic compounds.



Dr. Farah Aini Dahalan is currently a senior Lecturer in Universiti Malaysia Perlis, School of Environmental Engineering, Kangar, Malaysia. She received her BSc and MSc from Universiti Putra University, and her PhD. In Environmental Engineering from Universiti Teknologi Malaysia in 2011. Her interests include bioremediation, biodegradation, wastewater treatments, enzymology, microbiology, biochemistry, biotechnology and environmentally-related issues.